ABSTRACT

Title of Document: RESPONSE OF A THERMOACOUSTIC FLASHOVER DETECTOR TO THERMAL RADIATION

Zachary Tran Jeffrey
Master of Science, 2014

Directed By: Peter Sunderland, Associate Professor
Marino di Marzo, Professor
Department of Fire Protection Engineering

The thermoacoustic flashover detector is a device designed to be mounted on the helmet of a firefighter which creates a loud whistle when exposed to conditions that are consistent with flashover in order to provide firefighters with a warning and time to escape. The detector is based off a previous device designed at the University of Maryland which was operated using an electric band heater. This device was optimized by slightly altering the stack design and by the addition of approximately 0.3 mL of water to the stack, yielding an activation temperature of 125°C. Once the activation temperature was sufficiently lowered, the device was outfitted with copper fins which were designed to collect radiant heat from a propane-burning radiant panel and transfer it to the detector. When using four of these copper fins and exposed to a radiant heat flux of approximately 25 kW/m^2, the detector activated around 125°C after 7 minutes. This was the first known activation of a thermoacoustic device to unconcentrated thermal radiation. The response time of the device was lowered after two more fins were added to the design. Once the detector was shown to work using radiant heat, it was tested at the Maryland Fire and Rescue Institute (MFRI) at the University of Maryland using full scale fires in order to replicate the conditions in which it would be expected to operate. While the detector did not activate during the full scale tests, the radiant panel tests proved that the design is feasible and that some slight design changes are needed in order for the detector to operate in a real fire environment.

RESPONSE OF A THERMOACOUSTIC FLASHOVER DETECTOR TO THERMAL RADIATION

By

Zachary Tran Jeffrey

Thesis submitted to the Faculty of the Graduate School of the
University of Maryland, College Park in partial fulfillment
of the requirements for the degree of
Master of Science
2014

Advisory Committee:
Associate Professor Peter Sunderland, Chair
Professor Marino di Marzo
Professor Amr Baz

Acknowledgements

This research was made possible by the Department of Homeland Security Assistance to Firefighters Grant Program. I would like to thank Dr. Sunderland and Dr. di Marzo for giving me the opportunity to work on such a great project and for all of the assistance they've provided me throughout the course of my research. I would like to thank Olga Zeller for all of her assistance in the lab during this project and all of the other work that we've done together. I would like to that Marty LePore and all of the instructors at MFRI who assisted me during the full scale tests. I would like to thank Dan Gorham and Eric Link for being all the help they've given me, both in the classroom and during my research. I would also like to thank all of the faculty and staff in the Fire Protection Engineering department for making it such a great place to learn and work every day.

I would like to thank the Maryland Ultimate team. I can honestly say that without them, my entire college experience would have been completely different and I am grateful for all the experiences I was able to share with them.

Last and certainly not least, I would like to thank my parents and the rest of my family for supporting me and encouraging me to do whatever makes me happy. It's such a great feeling to know that you'll always be there for me no matter what. Thank you for everything that you've done for me.

Table of Contents

List of Tables

List of Figures

1 Introduction

Firefighting is generally considered one of the most dangerous occupations today due to the hazards to which firefighters can be exposed. These hazards can range from smoke and other toxic products of combustion, potential building collapse, intense radiant heat from fire, and flashover. While work has been done to improve firefighter turnout gear and firefighting operations from a tactical standpoint, thousands of injuries and many fatalities still occur every year. The National Fire Protection Association estimates that 69,400 firefighter injuries occurred in the line of duty and 31,490 injuries occurred during fireground operations in 2012 [1]. Additionally, there were 64 on-duty firefighter deaths in 2012 [2].

One of the most dangerous aspects of firefighting is when a compartment reaches flashover. This phenomenon is particularly dangerous because there are no obvious indicators that can predict when flashover might occur. As mentioned above, work has been done to improve other aspects of firefighting, so the purpose of this research project is to develop a thermoacoustic flashover detector for firefighters in order to give them some warning of impending flashover and provide them with enough time to reach a safe location. The phases of this research is including lower the activation temperature of the prototype device designed by Buda-Ortins, incorporating fins to transfer radiant heat designed by Hamburger, and testing the device with a radiant panel and in a fire environment to characterize the conditions needed for device activation.

1.1 Flashover

There are three stages in the life of a fire: the growth stage, fully developed stage, and decay stage. According to the International Standards Organization, flashover is defined as "the rapid transition to a state of total surface involvement in a fire of combustible material within an enclosure" [3]. More simply, flashover is the transition point from the growth stage to the fully developed stage of a fire which is accompanied by sudden and near-simultaneous ignition of all combustibles in a room. Figure 1-1 shows a generalized representation of the various stages of fire as well as the point at which flashover occurs.

Figure 1-1 Temperature variations during fire growth and decay [4]

While it is easy to visual tell when flashover occurs in a compartment, it is not easy to predict due to the varying conditions for which flashover can occurs; it is possible for flashover to occur when the compartment reaches temperatures in the range of 500-600°C or when the radiative heat flux to the floor reaches 15-20 kW/m^2 [4]. These types of environments because especially dangerous for firefighters not just because of the inherent danger of being in a room on fire but because their face pieces will likely fail after a short exposure [5]. Due to the enormous danger of being in a room during flashover, it is desirable to create a device that can "sense" the surrounding conditions and provide firefighters with ample warning to leave before the room reaches that point.

1.2 Thermoacoustics

Thermoacoustics is the joining of the fields of thermodynamics and acoustics. Thermoacoustic devices can be divided into two categories: engines, also known as prime movers, and heat pumps. The general idea of a heat pump is using sound waves to transfer heat from cold side of a pipe to the other, warmer side thereby creating a refrigerator. This works by sound waves compressing and moving packets

of gas from one side of a pipe to the other. Due to the compression, this packet of gas is now a higher temperature than its surroundings and therefore transfers its heat to that end of the pipe. As this packet moves back to the end that it started on, the sound waves expand the gas and absorb more heat from the starting end. The process is then repeated and results in a net transfer of heat from the starting end to the other end [6]. Thermoacoustic engines, or prime movers, on the other hand, create sound waves due to a temperature differential across the stack. This is the type of thermoacoustic device that will be examined and further developed for this research.

In general, thermoacoustic devices consist of a hot heat exchanger, cold heat exchanger, stack, and resonator, as shown in Figure 1-2. The stack is an essential part of the device because it provides a much larger surface area for heat transfer between the gas and the walls of the tube and heat exchangers [6]. As described above for the thermoacoustic refrigerators, heat is transferred by the compression and expansion, or rarefaction, of gas packets. The stack provides more surface area of heat transfer as well as a smaller distance for the gas packets to travel before transferring heat.

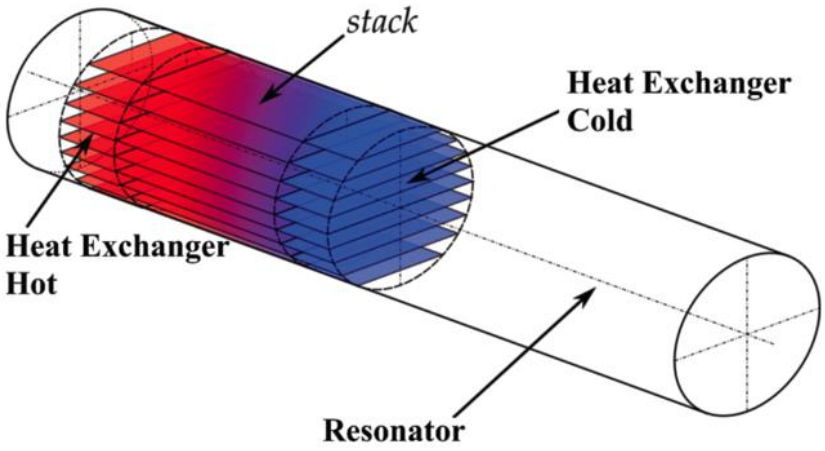

Figure 1-2 Typical arrangement of a thermoacoustic prime mover [19]

As their names would suggest, the hot heat exchanger is the location where heat is supplied to the device and the cold heat exchanger is the location where heat is removed or dissipated. A temperature gradient is created between the two heat exchangers as the heat added to the device is transferred across the stack and the fluid medium inside the device, which for this research is air. Once heat is added to the

device, it is transferred to the gas inside of the stack. As the heats up, it expands and creates an area of high pressure near the hot heat exchanger. These gas packets move towards the low pressure area by the cold heat exchanger where they contract and transfer heat. As gas contracts, the decrease in pressure moves the gas back towards the hot heat exchanger and the process is repeated. This process is shown in Figure 1-3. The gas packets do not have to oscillate from one end of the stack to the other, however. Instead, the gas packet oscillations are highly localized but numerous. The configuration of the stack allows for each gas packet to transfer heat over a small distance which improves the overall performance of the device. The oscillations of these gas packets is what causes the propagation of sound waves. This process, however, is impossible to sustain indefinitely as there is a minimum temperature gradient required for these oscillations to continue. As such, heat is required to be continuously added to the system to keep the temperature gradient above a certain critical point, otherwise the temperature gradient across the stack will diminish to the point where the oscillations will stop and the device will stop producing sound [20]. It is also important to note that the temperature of the gas does not match the temperature of the stack; the gas by the hot heat exchanger is slightly cooler than the stack and the gas by the cold heat exchanger is slightly warmer than the stack, as shown in Figure 1-3.

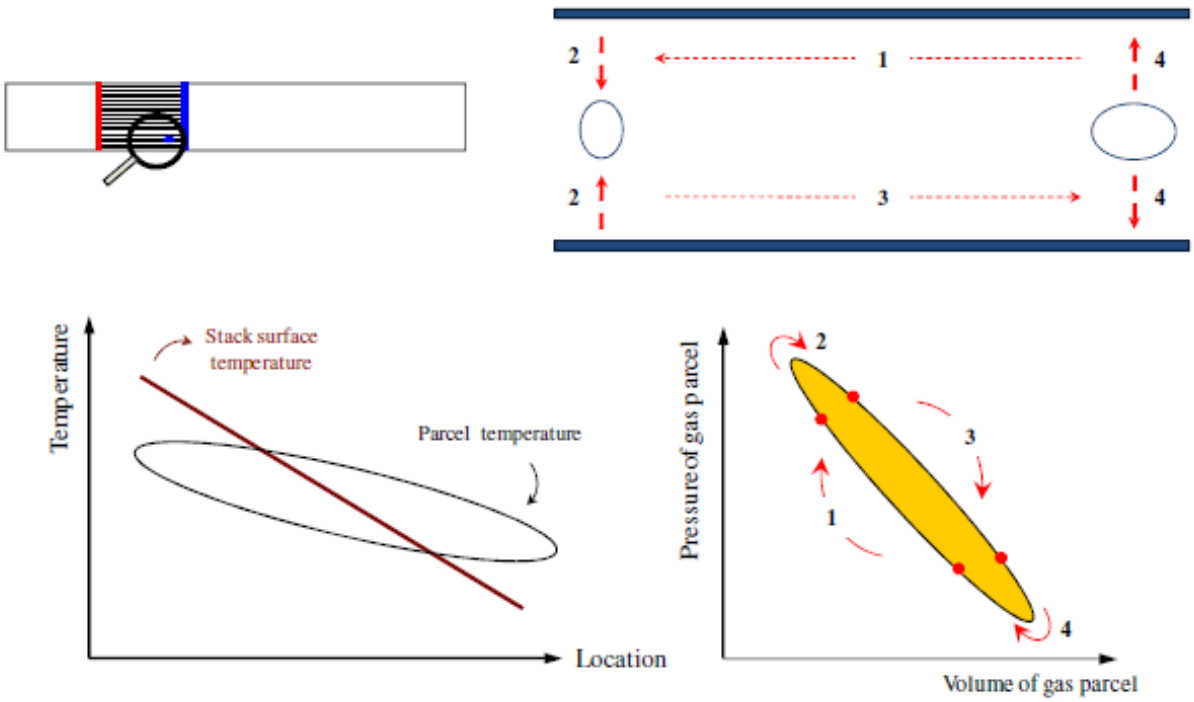

Figure 1-3 Operational process of a standing wave thermoacoustic engine [18]

1.3 Previous Work

The current prototype device was designed based off of some preexisting thermoacoustic engines, utilizing similar dimensions and materials. The most influential of these designs come from Jung and Matveev [8], Smoker et al. [9], and Wheatley et al. [10], though there have been other designs for thermoacoustic engines such as the one by Raspet et al. [11] and Symko et al. [12]. Chen and Garrett further simplified their thermoacoustic engine by powering it with concentrated solar radiation [13].

Jung and Matveev's device consisted of two flanged copper tubes, one open and one closed, ceramic and copper fittings, and a pressure transducer, as shown in Figure 1-4. In addition, graphite gaskets were used to minimize any leakages. The ceramic fitting was chosen as the stack holder in order to minimize the heat transfer between the hot and cold heat exchangers whereas copper was used everywhere else for its high heat conduction. Not pictured in Figure 1-4 are the two copper mesh heat exchangers they placed on both sides of the stack. They used an electric band heater or a butane torch as their heat inputs and used a water-cooled jacket to cool the other end of the device. For the stack itself,

Jung and Matveev utilized a reticulated vitreous carbon (RVC) open-cell foam with 80 pores-per-inch. One of the important things that Jung and Matveev noticed with their experiments is that the critical temperature difference was dependent on the length of the device and the position of the stack within the device. Additionally, they noticed that the acoustic frequency output increases as engine length decreases, 1.7 kHz for the 67 mm engine and 0.94 kHz for the 124 mm engine. The lowest critical temperature difference that they observed was 213°C for an engine length of 100 mm and the greatest critical temperature difference was 288°C for an engine length of 57 mm [8].

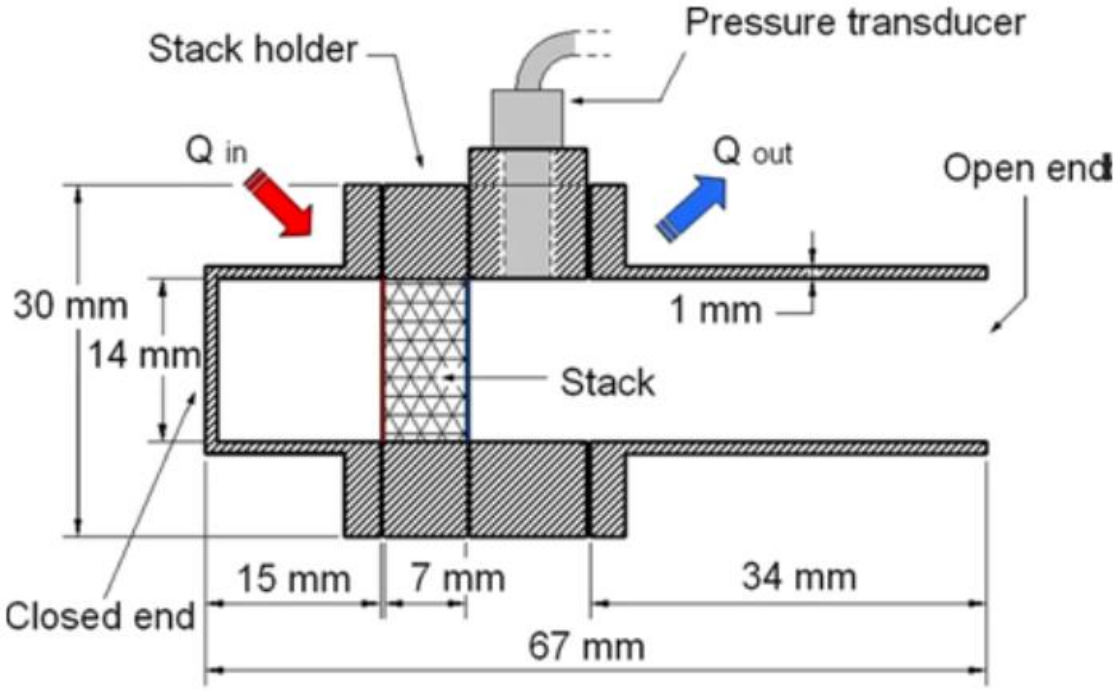

Figure 1-4 Schematic of Thermoacoustic Engine Designed by Jung and Matveev [8]

The device designed by Smoker et al. was incredibly important to this project because the original prototype design by Buda-Ortins was based off of these dimensions. Smoker et al. were able to create a thermoacoustic device using a Pyrex tube as a resonator, having a length of 175 mm and inner diameter of 20 mm. Instead of using an external heating source attached to a heat exchanger, Smoker et al. utilized a resistance wire that zig-zagged across the inside of the tube to provide heat internally to the stack. In addition, they did not use a cold heat exchanger. This device was able to produce sound at a frequency of 500 Hz from an input of 33 W [9].

The thermoacoustic engine designed by Wheatley et al. differs in numerous ways from the design of Jung and Matveev. This design consists of two copper tubes, the open tube being 144 mm long and the closed tube being 131 mm long. A 20 mm long stack constructed from fiberglass strips was placed between the two copper pipes. Whereas Jung and Matveev used a stack holder made from ceramic, Wheatley et al. used a stainless steel with poor thermal conductivity. Figure 1-5 provides a simple schematic of their device. While the operation of the engine is fundamentally the same, the procedure that Wheatley et al. used is the complete opposite from Jung and Matveev. Instead of heating the closed end of the tube, they submerged the open end in liquid nitrogen while leaving the closed end around ambient temperature. This process resulted in frequencies around 200 Hz [10]. An important distinction between this device and the device designed by Jung and Matveev is that this device does not incorporate heat exchangers in its design.

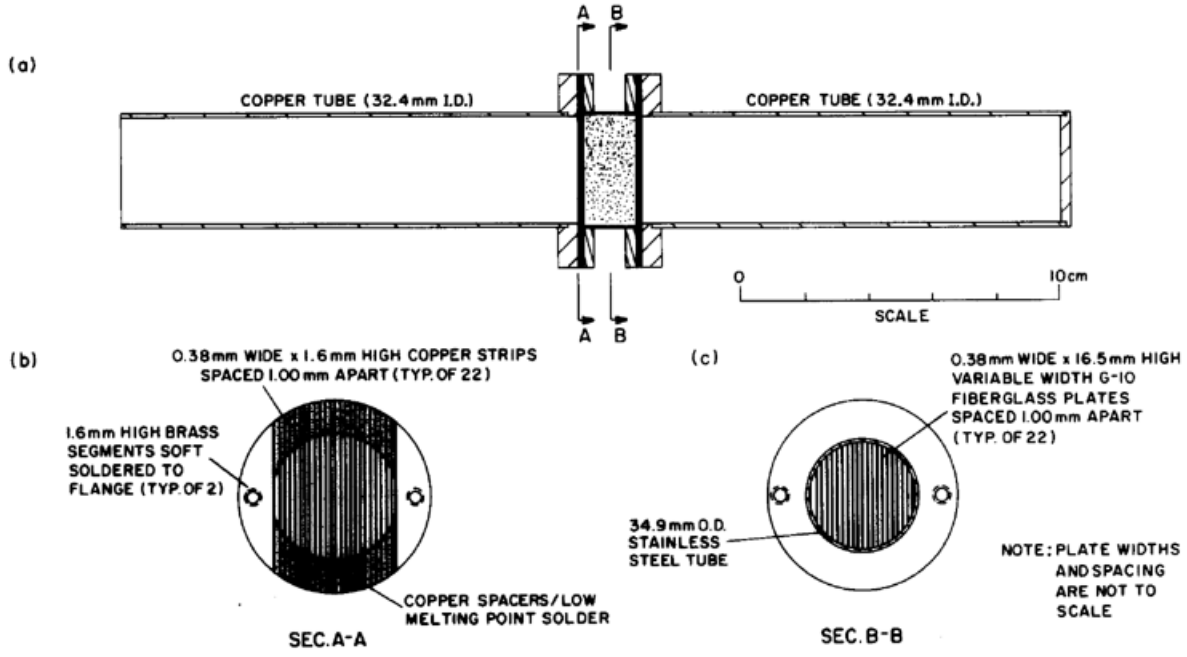

Figure 1-5 Schematic of Thermoacoustic Engine by Wheatley et al. [10]

The device designed by Raspet et al. was much larger than the rest, measuring 72.7 cm long with a radius of 4.32 cm. The entire device was made entirely out of copper with the exception of the stack which was a ceramic sample of a monolithic catalyst support with square pores that ran parallel to the

device. The heat exchangers for this device were made from copper strips, arranged in a similar manner as the ceramic stack in the device designed by Wheatley et al. For some of their experiments, an impedance tube was attached to the end of the device in order to measure the specific acoustic impedance of the device. A simple diagram of this device is shown in Figure 1-6. Heat was supplied to the device by wrapping high temperature heat tape around the entire top section of the device and then insulating it. When the impedance tube was removed, the device produced a frequency of 115 Hz with a temperature difference of 176 K [11].

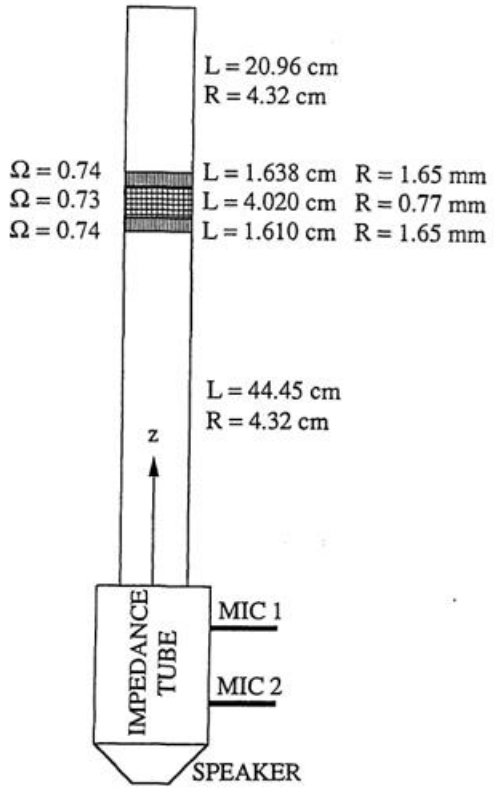

Figure 1-6 Thermoacoustic Engine Designed by Raspet et al. [11]

The device designed by Symko et al. is on the opposite end of the spectrum, in terms of size, compared to the device from Raspet et al., measuring 2 cm long. This device was designed to remove heat from a circuit by using the heat to produce sound. At sound onset, a temperature difference of 40°C was measured from a 2 W input, producing a frequency of approximately 2 kHz [12].

Chen and Garrett used a much different approach to heating their thermoacoustic device. While they still used a ceramic stack, copper cold heat exchanger, and copper resonator with a removable Lucite tube, they did not use a hot heat exchanger and the closed end cap was made from a Pyrex beaker. A schematic of their device is shown in Figure 1-7. Instead of using an electric heater or heat tape, Chen and Garrett designed this device to operate based on concentrated solar radiation. Using a 35 inch diameter, 30 inch focal length Fresnel lens, they were able to concentrate the sun's radiation into a 7 cm diameter spot on the stack in place of a hot heat exchanger. With this method, they were able to produce 275 W and measured sound onset at 35 W at a frequency of 420 Hz [13].

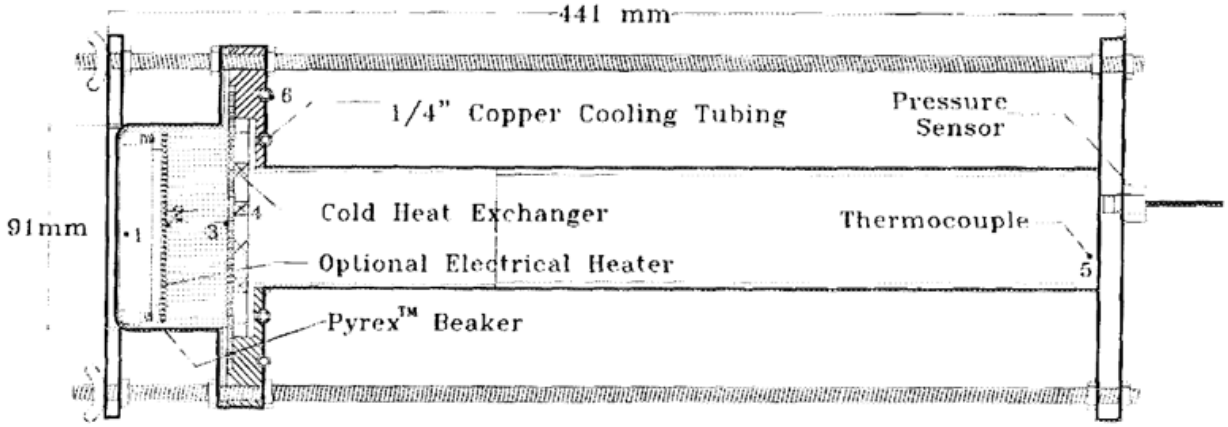

Figure 1-7 Thermoacoustic Device Designed by Chen and Garrett without Fresnel Lens [13]

Jin et al. briefly examined how any inclination in the device would affect its onset temperature, in addition to other experiments such as determining optimum stack position in the device. Once they found the optimum stack position for their device, they tested it at varying angles, from 90 to -90 degrees where 90° corresponds to having the open end upward and -90° corresponds to the open end downward. They found that the minimum onset temperature for their thermoacoustic prime mover occurred when the device was horizontal and increased as the device was rotated in either the positive or negative direction. They attribute this variation in onset temperature to the affect that the inclination has on natural convection [16]. Their findings are shown in Figure 1-8.

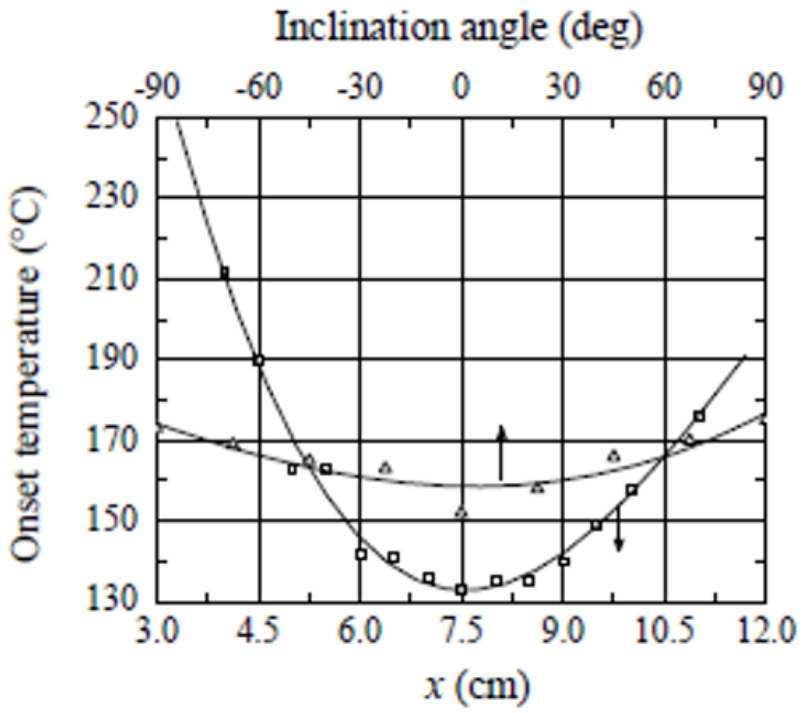

Figure 1-8 Effect of Stack Position and Inclination on Thermoacoustic Device by Jin et al. [16]

1.4 Overview of Work by Buda-Ortins

The starting point of this research project was the work done by Buda-Ortins in constructing a working prototype thermoacoustic device based on some of the designs mentioned in the previous section. Buda-Ortins constructed two prototype devices; Figure 1-9 shows what this prototype device looked like and the details of the most successful design are given in Table 1-1. It is important to note that the dimensions shown in Table 1-1 are the dimensions of each component as seen from the exterior. Each component has a lip so that components can fit together and accommodate graphite gaskets. Even though the stack holder appears to be 6.4 mm long, it is 12.7 mm long in actuality in order to include a lip on each side of the component. Conversely, while the heat exchangers appear to be 12.7 mm long, the copper foam only occupies the middle 6.4 mm of the component. Thin graphite gaskets were used at each junction in order to eliminate any air gaps with the exception of the junction between the cold heat exchanger and the aluminum resonator tube. This particular junction was sealed using Permatex RTV sealant. As shown in Figure 1-9, the device is held in compression between two aluminum plates; a thin

sheet of rubber is placed between the MACOR end cap and the bottom aluminum plate to avoid any damage to the end cap, and the aluminum resonator is threaded and attached to the top aluminum plate. For the stack material, Buda-Ortins used steel wool which was rolled into a ball with an approximate density of $\rho = 156$ kg/m^3 [14].

Buda-Ortins used an electric band heat to supply heat to the device, the same method as Jung and Matveev. In addition, a Variac transformer was used to vary the power supplied to the heat band. In order to cool the cold heat exchanger, Buda-Ortins included a Styrofoam cup into the design, which can be seen in Figure 1-9. A hole was cut in the bottom of the cup and was inserted into the design between the stack holder and the cold heat exchanger. The cup was used to hold ice around the cold heat exchanger.
Buda-Ortins' most successful designed required an input of 47 W, which resulted in a hot heat exchanger temperature of 267°C and cold heat exchanger temperature of 169°C yielding a critical temperature difference of 105°C and sound frequency of 640 Hz.

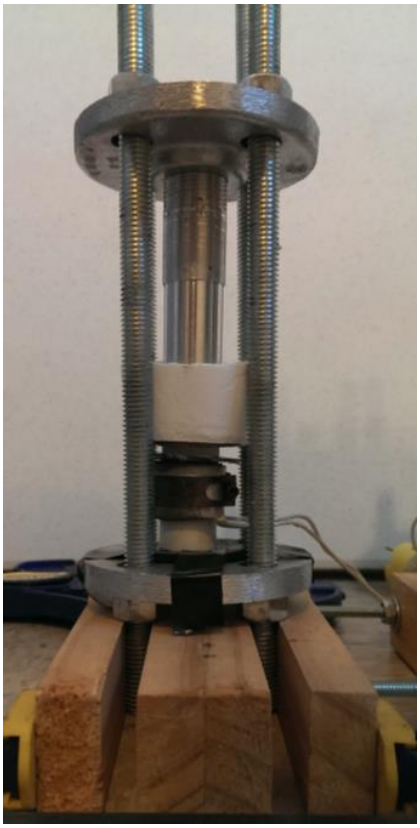

Figure 1-9 Prototype Device Designed by Buda-Ortins, reproduced from Hamburger [7]

Table 1-1 Dimensions and Materials of Components in Prototype Device [14]

Component	Length (mm)	Inner Diameter (mm)	Outer Diameter (mm)	Material
End Cap	25.4	20.3	25.4	MACOR
Hot Heat Exchanger	12.7	22.4	25.4	Copper Foam
Stack Holder	6.4	20.3	25.4	MACOR
Cold Heat Exchanger	12.7	22.4	25.4	Copper Foam
Resonator	101.6	20.3	25.4	Aluminum

1.5 Overview of Work by Hamburger

Hamburger continued the work done by Buda-Ortins to construct a prototype thermoacoustic flashover detector. Since Buda-Ortins had already developed a prototype thermoacoustic device, the majority of Hamburger's work was to optimize its dimensions in order to bring down the hot heat exchanger temperature and critical temperature difference required for sound onset to occur. Hamburger looked at optimizing temperature, power consumption, device complexity, and cost [7].

In the first attempt at optimization, Hamburger removed the cold heat exchanger from the device, hoping that the aluminum resonator would be a sufficient heat sink and that the device would be reliable due to the fewer number of junctions in the device. During this span of tests, Hamburger varied numerous things, including the overall length of the device as well as the density of the stack. None of these changes failed at improving the original design.

The next set of attempts involved varying the inner and outer diameters of each component but leaving the overall length unchanged. This led to two more prototypes, as shown in Figure 1-10. While

both new prototypes failed to produce any sound on their own, Hamburger noticed that the larger of the new devices was able to sustain a sound if tapped. However, the device was only to hold this forced resonation when the hot heat exchanger was above 300°C.

Figure 1-10 Exploded View of Prototype Devices with Varying Diameters [7]

One of the primary enhancements made by Hamburger was the discovery that the inclusion of water lowered the activation temperature of the device, activating at 285°C instead of the 308°C that Buda-Ortins had experienced. The decreased activation temperature was believed to be due to the fact that the expansion of evaporating water is orders of magnitude greater than the expansion of heated air. Hamburger found that the lowest temperature needed on the hot heat exchanger for activation was that found from using Buda-Ortins original device with the inclusion of 1-2 mL of water on the stack. Hamburger measured the current drawn by the band heater as a function of output voltage from the Variac transformer, shown as Figure 1-11, in order to calculate the power required to activate the device. Based on this, Hamburger determined that a minimum of 22 W was required for sound onset and that sound could be sustained with 12 W.

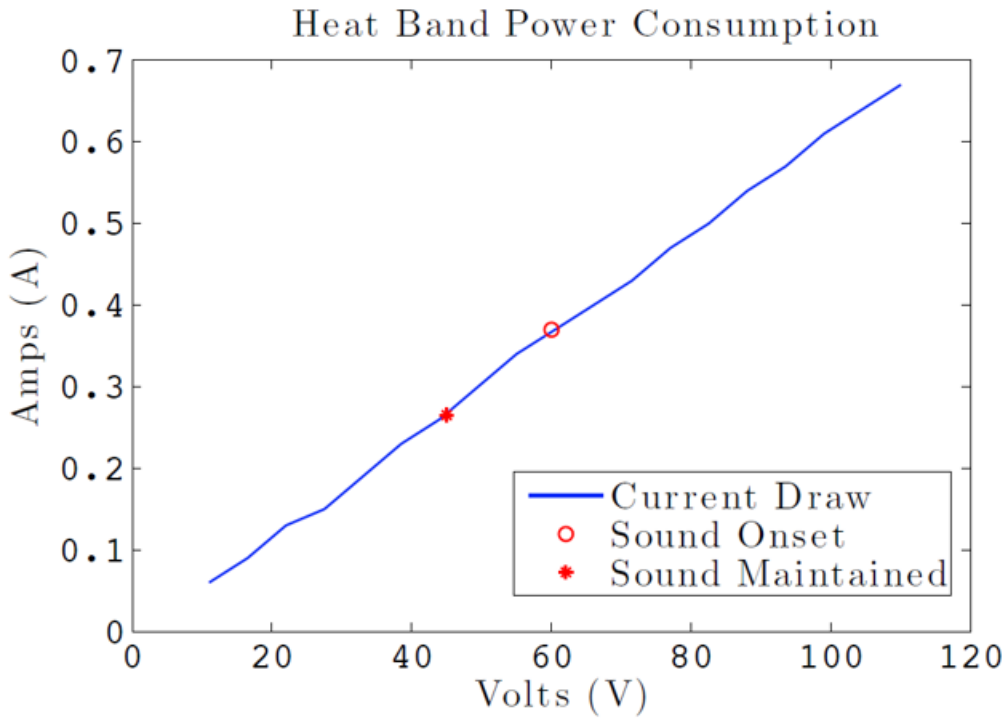

Figure 1-11 Amperage Drawn by Band Heater vs. Variac Output Voltage [7]

Hamburger also performed an extended surface heat transfer analysis in preparation to collect radiant heat to transfer to the device. In order to collect radiant heat, Hamburger designed and built copper fins, using copper due to its heat transfer properties. In order to transfer the heat from the fins to the device, Hamburger utilized heat pipes that ran through the center of the fins, a diagram of which is shown in Figure 1-12. To improve the heat transfer from the copper fins to the heat pipe, Hamburger inserted thin pieces of copper wire as well as used a thermally conductive epoxy to increase surface contact. The copper fins measured 10 cm along the heat pipe, protruded 5 cm on each side, and were 1.6 mm thick. The heat pipes themselves were 17.8 cm long with a 5 mm diameter. The section that was not contained within the copper fin was bent such that the last 1.27 cm of pipe would be in contact with the hot heat exchanger. Hamburger produced three fin/heat pipe collectors but was unable to incorporate them into the prototype designed by Buda-Ortins.

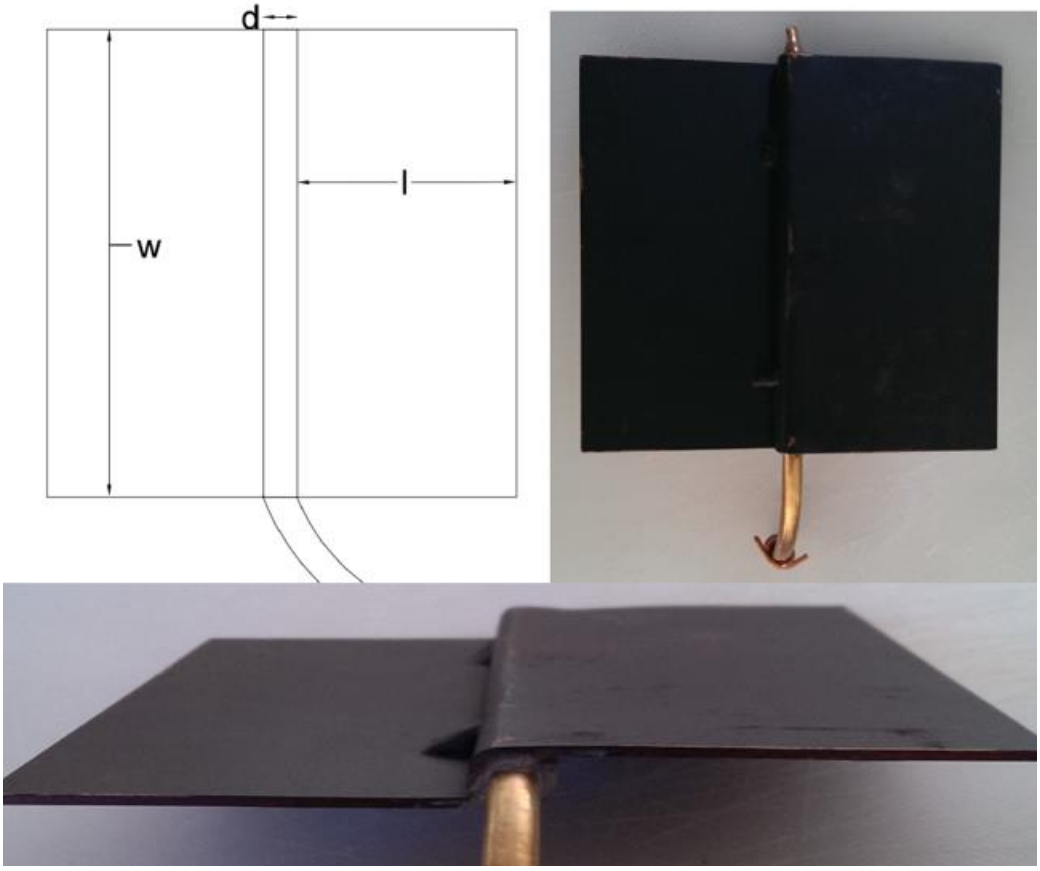

Figure 1-12 Diagram, Top, and Side View of Fin/Heat Pipe Collector [7]

1.6 Objectives

The goals of this research are threefold: the first is to bring down the temperature of the hot heat exchanger at onset to 200°C or lower; the second is to incorporate fins into the device in order to achieve sound onset using radiant heat; and the third is to test the device in a full scale fire scenario and achieve sound onset. The first goal is necessary because a flashover detector would be very useful to firefighters if it had to reach 300°C before activating. The second goal is necessary prior to testing in a full scale fire scenario in order to prove that the device can work using radiant heat in a lab setting. In other words, it needs to work in a controlled environment. The third goal is the true goal of this research because it would show that the device would work in environments that firefighters would be subjected to.

2 Testing Stage 1: Electric Band Heater

2.1 Motivation and Objectives

The end goal of this project is to building a prototype thermoacoustic flashover detector that would be mountable on firefighter helmets. Buda-Ortins was able to develop a thermoacoustic device but was unable to proceed any further. Hamburger attempted to optimize and reduce the size of the device designed by Buda-Ortins but found that any reduction in size required a greater heat input in order to activate the device. However, Hamburger did find out that the addition of water reduced the activation temperature of the device. Additionally, Hamburger was able to design and build fin/heat pipe collectors that could be used to transport radiant heat to the device but was unable to incorporate them into the device. Before it was worthwhile to incorporate the fins into the device, it was desired to lower the required activation temperature of the device to around 200°C at the hot heat exchanger. Instead of trying to alter large components of the device as Hamburger attempted, the stack material and amount of water applied to the stack was varied.

2.2 Methods

The various stack materials that were tested consisted of steel wool, stainless steel wool, bronze wool, aluminum wool, and a ceramic honeycomb material similar to the one used by Raspet et al. [11] and Chen and Garrett [13]. The wool strands varied in thickness, being either fine, medium, or coarse. The steel wool that was tested was the original steel wool used by Buda-Ortins and Hamburger and was Grade 3 steel wool.

One of the biggest changes between the first steel wool tests and the later ones was the amount of water that was added to the stack. As mentioned in the previous section, Hamburger added 1-2 mL of water to the stack. The overall performance of the device improved when the amount of water was cut to about 0.3 mL. As Hamburger explained, the addition of water effectively jump-starts the cycles of compressions and rarefactions in the stack because the expansion of evaporating water is much greater

than air. The addition of less water decreases the amount of energy needed to heat the water to its boiling point which in turn decreases the time to activation and decreases the required activation temperature. The low measured activation temperature in these tests is possible due to the high heat transfer of the copper to the stack.

Once the optimum conditions for the stack material and amount of water was determined, tests were conducted using a Variac variable transformer to adjust the input voltage to the band heater in order to determine the lowest power requirement necessary to activate the device. The voltages were varied starting at 100V and decreased in increments of 10V for each test. The heater used was model MB1A1A1A3 from Omega and has a power density of 0.0744 W/mm^2 at a voltage of 120V [15]. The area of the heat exchanger in contact with the band heater was measured to be 911 mm^2, which is not quite the full surface area of the heat exchanger because of a small gap in the band heater. The amount of heat transferred to the heat exchanger is scaled as a function of the voltage squared because the heater acts as a resistor in the equation $P = V^2/R$. Based on this analysis, the heat transferred is the theoretical amount that should be transferred, however, the actual amount may vary slightly. Two Type K thermocouples were used to measure the temperature on the outside of the hot heat exchanger and on the inside of the cold heat exchanger. Due to the porosity of the cold heat exchanger, it was hard to maintain good contact with the thermocouple probe. For each of these tests, the cold heat exchanger was kept cold by a single ice cube held in a Styrofoam cup around the heat exchanger.

2.3 Results and Conclusions

Table 2-1 details the various tests done with these different materials, outlining the mass of the stack, whether water was added, whether the device activated, and the temperature of activation. The temperatures noted in Table 2-1 are the temperatures measured on the outside of the hot heat exchanger. The density shown in Table 2-1was calculated by dividing the mass by the volume of the stack holder, approximately 4.11 cm^3. Based on these few tests, the original steel wool and fine bronze wool required the lowest activation temperature. While the bronze wool stack had the lowest activation temperature at

113°C, it was not consistently repeatable. However, it still required a much lower onset temperature than found by Buda-Ortins and Hamburger. During these tests, the lip of the stack holder became chipped. Once the stack holder was replaced with a new one, the original steel wool demonstrated much lower activation temperatures as well. As shown in the table below, the steel wool tests were much more consistent. Based on these results the steel wool was chosen as the stack material for the rest of this project. It may be possible to optimize a fine bronze wool stack for more consistent activation temperatures in future research.

Table 2-1 Device Activation Using Different Stack Materials

Material	Mass (g)	Density (kg/m^3)	Water Added	Activation	Temperature (°C)	Notes
Original Steel Wool	0.71	172.7	Yes	Yes	307	
Original Steel Wool	0.71	172.7	Yes	Yes	297	
Fine Bronze Wool	0.7	170.3	No	Yes	373	
Fine Bronze Wool	0.7	170.3	Yes	Yes	113	
Fine Bronze Wool	0.7	170.3	Yes	Yes	174	
Medium Bronze Wool	0.73	177.6	Yes	Yes*	335	Tapped start
Medium Bronze Wool	0.7	170.3	Yes	Yes	332	
Medium Bronze Wool	0.56	136.2	Yes	Yes	326	
Coarse Bronze Wool	0.68	165.4	Yes	Yes	325	
Coarse Bronze Wool	0.49	119.2	Yes	No		
Fine Aluminum Wool	0.36	87.6	No	No		
Fine Aluminum Wool	0.36	87.6	Yes	No		
Fine Aluminum Wool	0.73	177.6	No	No		
Fine Stainless Steel Wool	0.65	158.1	No	Yes	382	
Fine Stainless Steel Wool	0.65	158.1	Yes	Yes*	315	Tapped start
Ceramic	1.8	437.9	No	Yes	437	
Ceramic	1.8	437.9	No	Yes	366	
Ceramic	1.8	437.9	Yes	Yes	395	

Original Steel Wool	0.73	177.6	Yes	Yes	136	New stack holder, previous holder was chipped
Original Steel Wool	0.73	177.6	Yes	Yes	135	
Original Steel Wool	0.73	177.6	Yes	Yes	118	
Original Steel Wool	0.73	177.6	Yes	Yes	105	

Table 2-2 provides the results from the tests varying the input voltage. The data from the 70V test is not included due to the thermocouple losing contact with the heat exchangers. As Table 2-2 shows, the required temperatures on the hot and cold heat exchangers for sound onset remains fairly consistent for all of these tests. Figures 2-1 through 2-6 show how the temperature at each heat exchanger changes over the duration of each test as well as indicates the time when sound onset occurs. The point at which the hot heat exchanger begins to drop coincides with turning off the power to the band heater. While the lowest temperature difference at onset was measured as 30°C at 40V, the power requirement was deemed too low for the device because the activation time was too long. Since the desired activation time is around 2 minutes, a power requirement of approximately 30 W would be necessary to activate the device.

Table 2-2 Device Characteristics at Sound Onset for Different Voltage Inputs

Voltage (V)	**Power (W)**	**Sound Onset (mm:ss)**	**Temperature Difference (°C)**	**Hot (°C)**	**Cold (°C)**
100	47	01:37	91	126	35
90	38	02:00	133	139	6
80	30	01:36	103	111	8
60	17	03:10	91	107	16
50	12	05:36	100	112	12
40	8	15:54	30	106	76

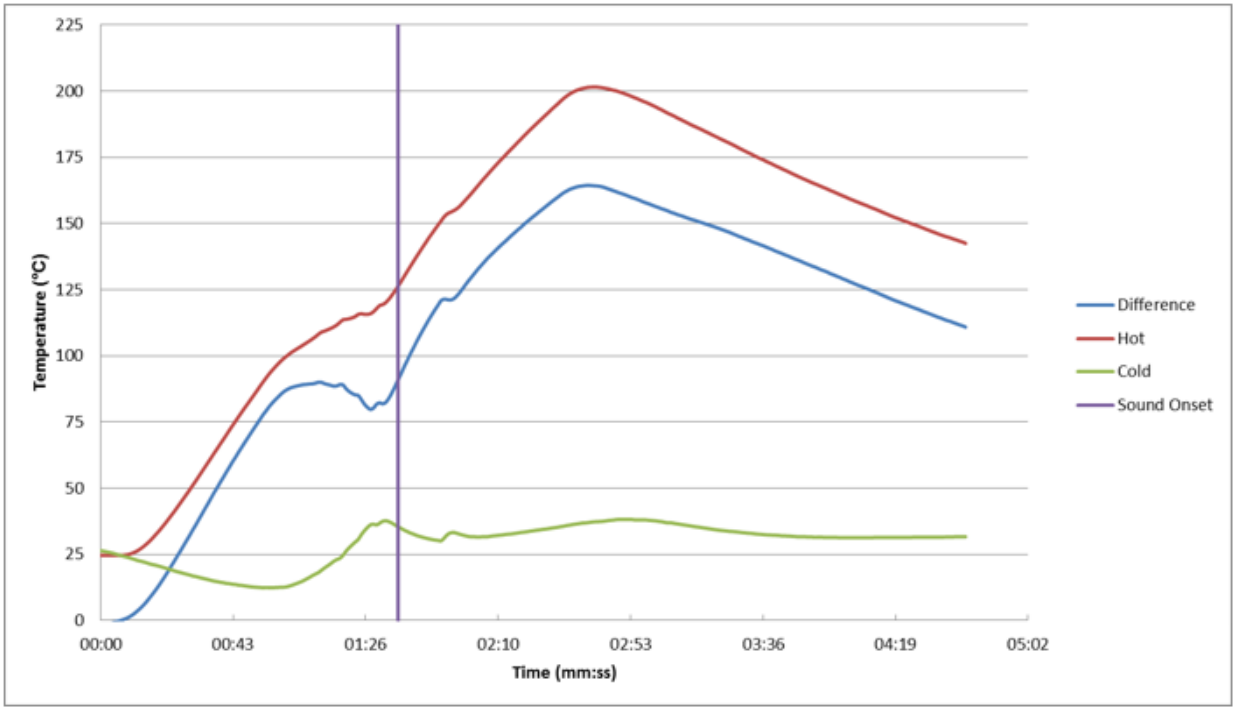

Figure 2-1 100V Band Heater Temperature Data

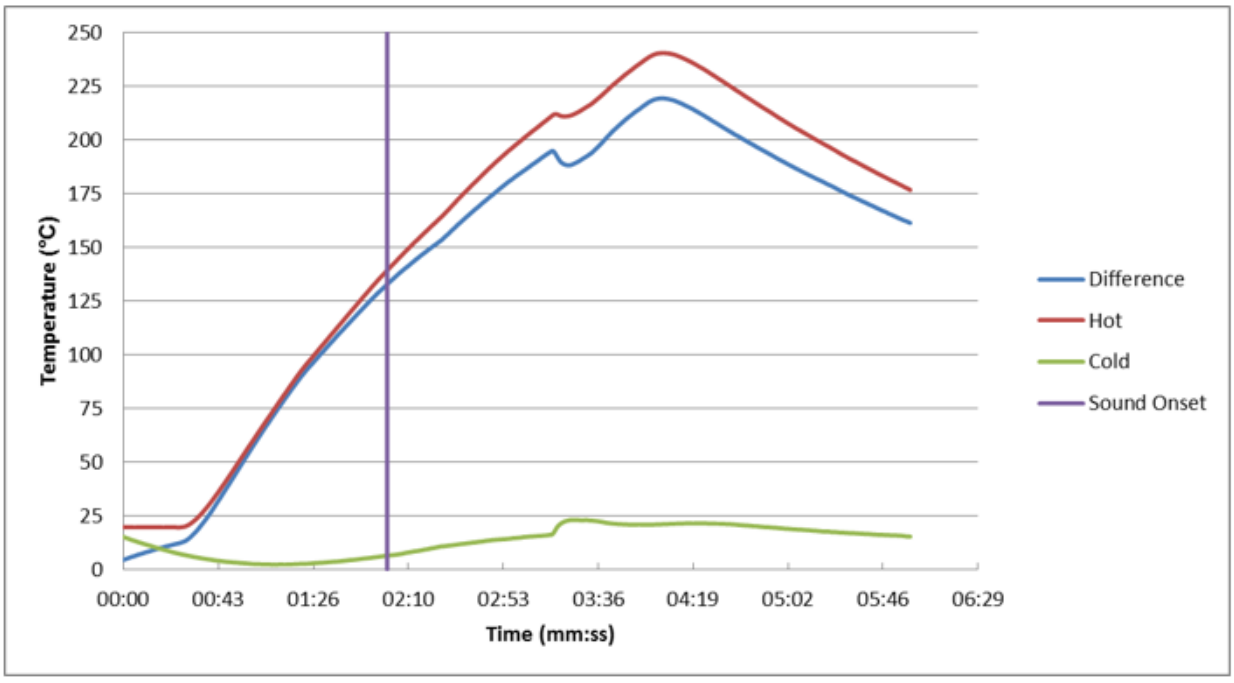

Figure 2-2 90V Band Heater Temperature Data

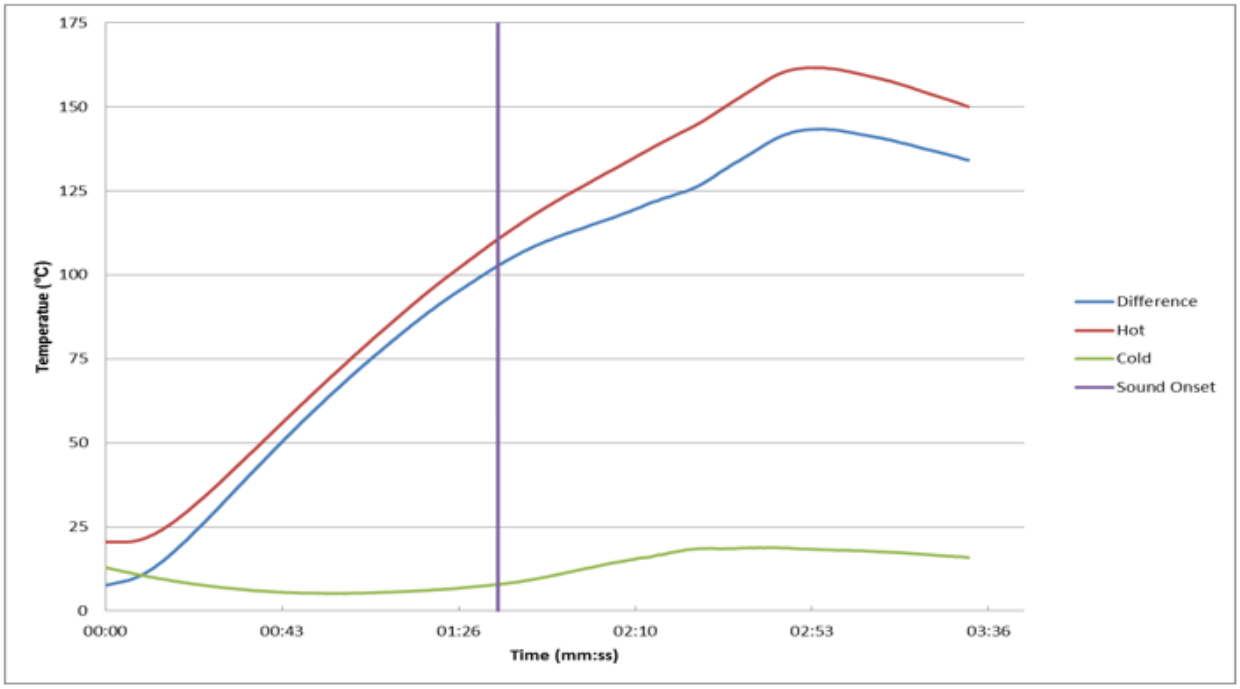

Figure 2-3 80V Band Heater Temperature Data

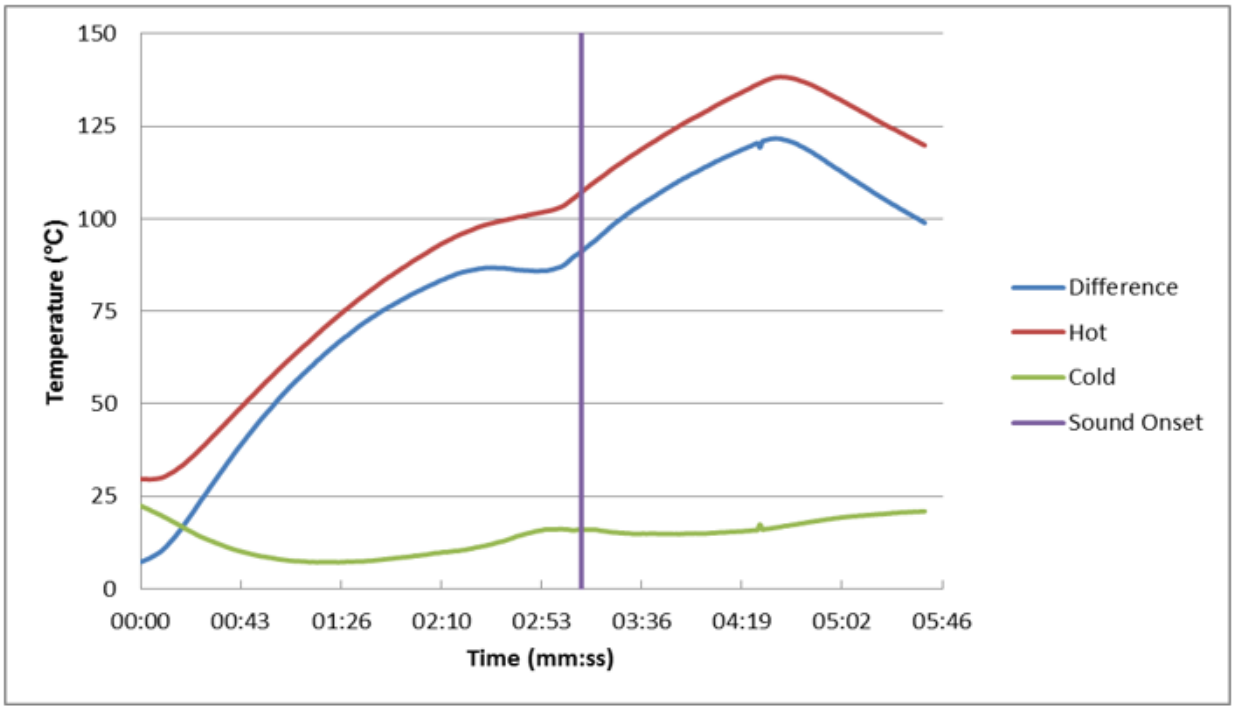

Figure 2-4 60V Band Heater Temperature Data

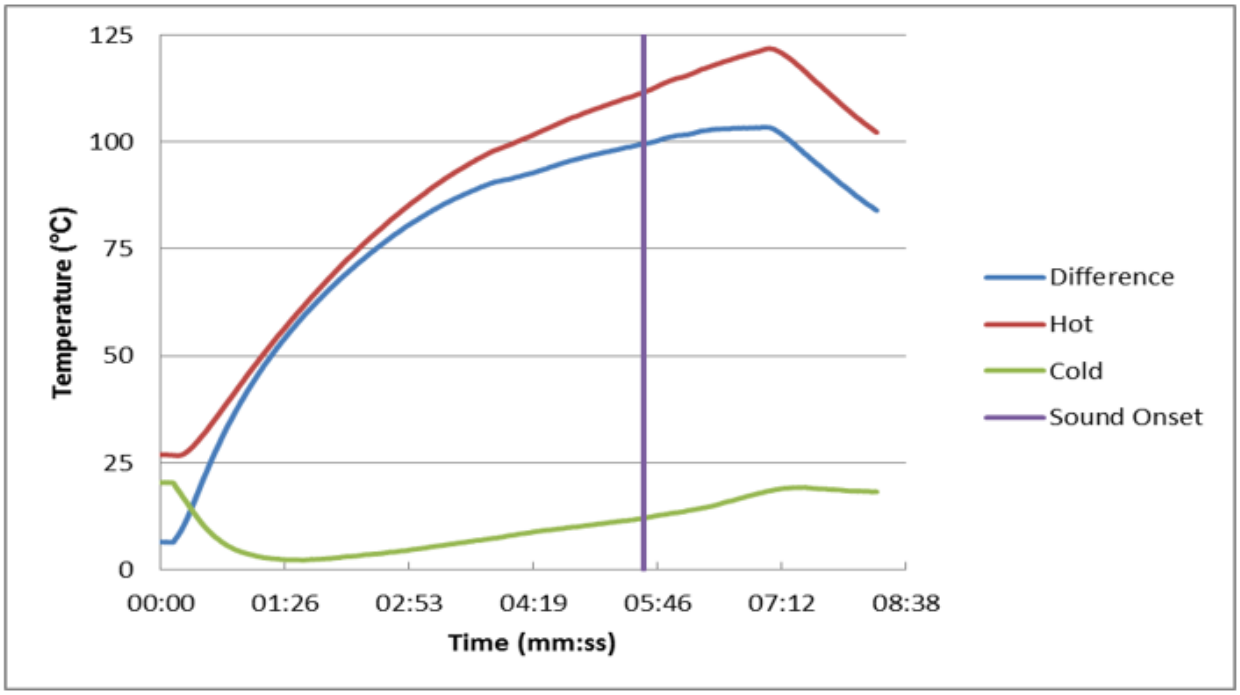

Figure 2-5 50V Band Heater Temperature Data

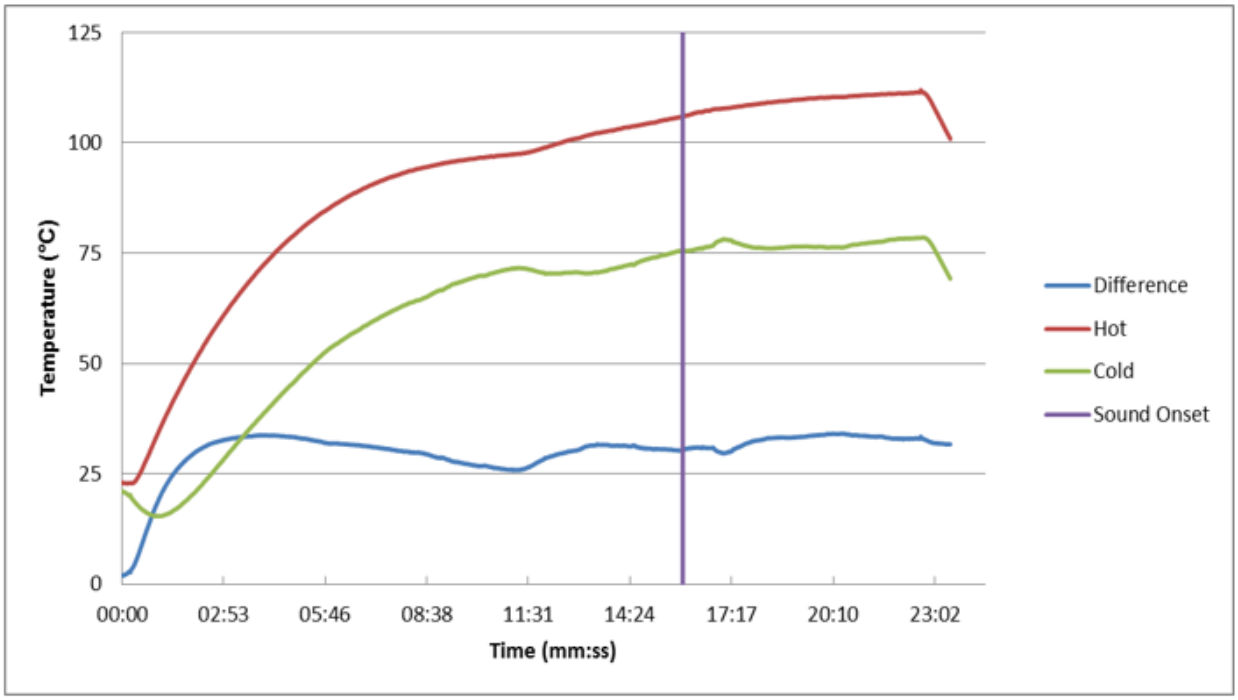

Figure 2-6 40V Band Heater Temperature Data

3 Testing Stage 2: Radiant Panel

3.1 Motivation and Objectives

Although the large decrease in activation temperature was a huge advancement from the results of Buda-Ortins and Hamburger, the final goal of the project is to create a prototype device that works using radiant heat so that it can activate if worn on a firefighter helmet in a fire. Once the device was shown to activate consistently at much reduced temperatures, around 115°C, the next step in the project was to prepare the device to work using radiant heat instead of using an electric band heater and testing the device using a radiant panel before testing in a full scale fire scenario.

3.2 Methods

During his research, Hamburger design and built three prototype fins that he envisioned using to collect radiant heat from a fire and smoke layer and to transfer that heat to the device. The fins themselves were made from a 1.6 mm copper sheet, measured a total 10 cm x 10 cm, and were painted black to maximize their absorptivity. The copper fins then wrapped around a portion of a heat pipe in order to transfer the heat from the fins to the hot heat exchanger of the device. Heat pipes were used to transfer heat instead of solid metal rods because heat pipes are more efficient due to the fact that the transfer heat through conduction and phase transition. The heat pipe itself is a thermally conductive casing, a wick, and a vapor cavity. The wick is typically some sintered metal powder or a series of parallel grooves that exerts capillary pressure on the condensed working fluid of the heat pipe. The working fluid of the heat pipe can be any fluid that undergoes phase change and can be selected to provide optimal performance for its use. The heat pipes used in the development of the collectors is made with a copper casing and water as the working fluid. As heat is added to one end of the pipe, it is transferred to the cool end of the pipe via conduction along the copper casing and through the phase transition of the working fluid inside the pipe. As the water inside the pipe evaporates due to the added heat, the vapor moves down the heat pipe through the vapor cavity towards the cool side of the pipe. The vapor then transfers heat to the cool end of

the pipe and condenses. After condensing, the fluid moves back towards the hot end of the pipe through the wick by capillary action. This process is shown and described in Figure 3-1. The majority of heat transfer is done through this phase transition process.

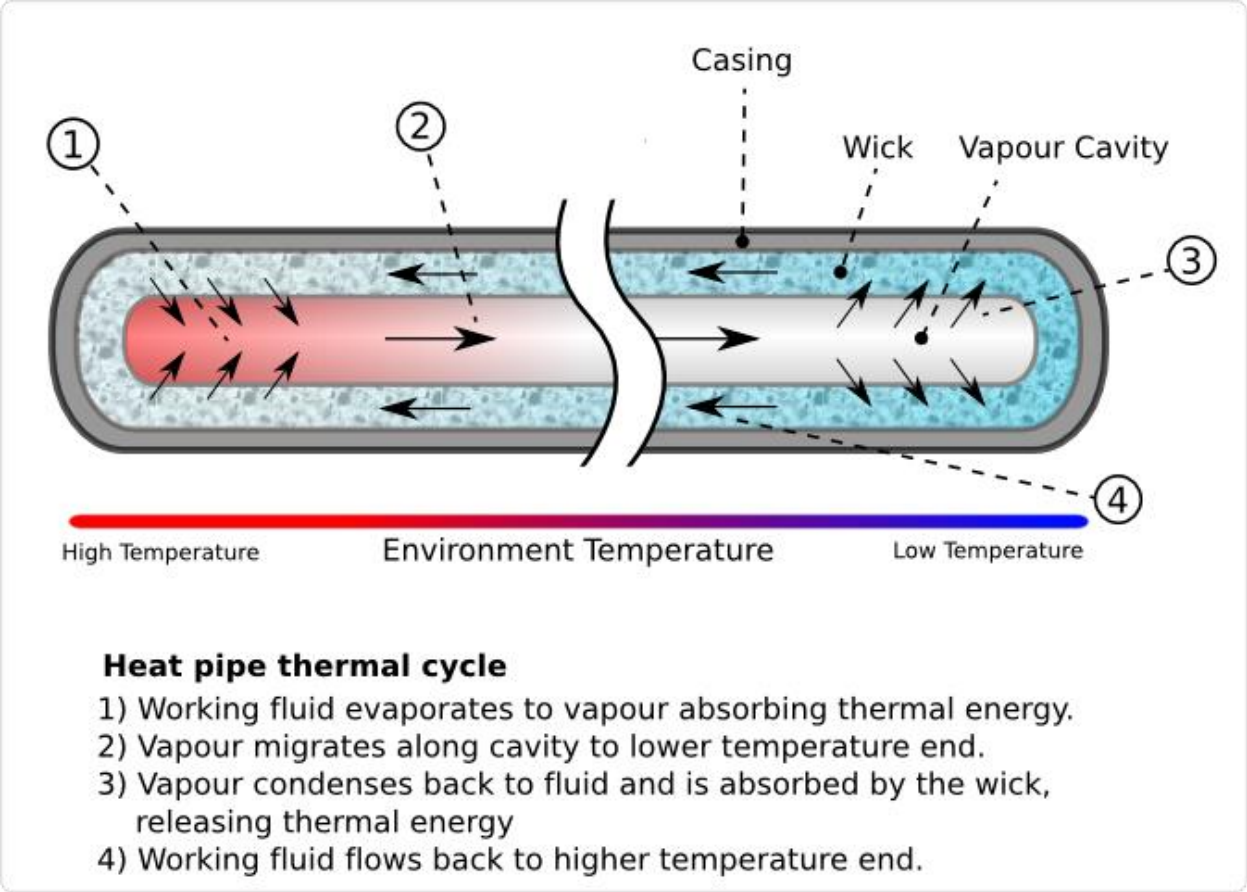

Figure 3-1 Components and Operation of a Heat Pipe [21]

A thermally conductive epoxy was applied and thin copper wires were inserted between the heat pipe and the fin in order to maximize the contact area and heat transfer. The heat pipes were bent 90° so that the end of the heat pipe would have a maximum contact area with the hot heat exchanger while the fins were oriented perpendicular to the length of the device, thereby maximizing the area which can be exposed to radiant heat from the smoke layer. From the prototypes built by Hamburger, a fourth fin was created to increase the amount of heat transferred to the device as well as make it symmetric. The symmetry of the fins was desirable because of the threaded rods around the device used to keep it in compression; spacing four fins around the device was easier than spacing three fins and provided a more

uniform temperature distribution along the hot heat exchanger. Figure 3-2 shows how the fins are arranged looking at the bottom of the device.

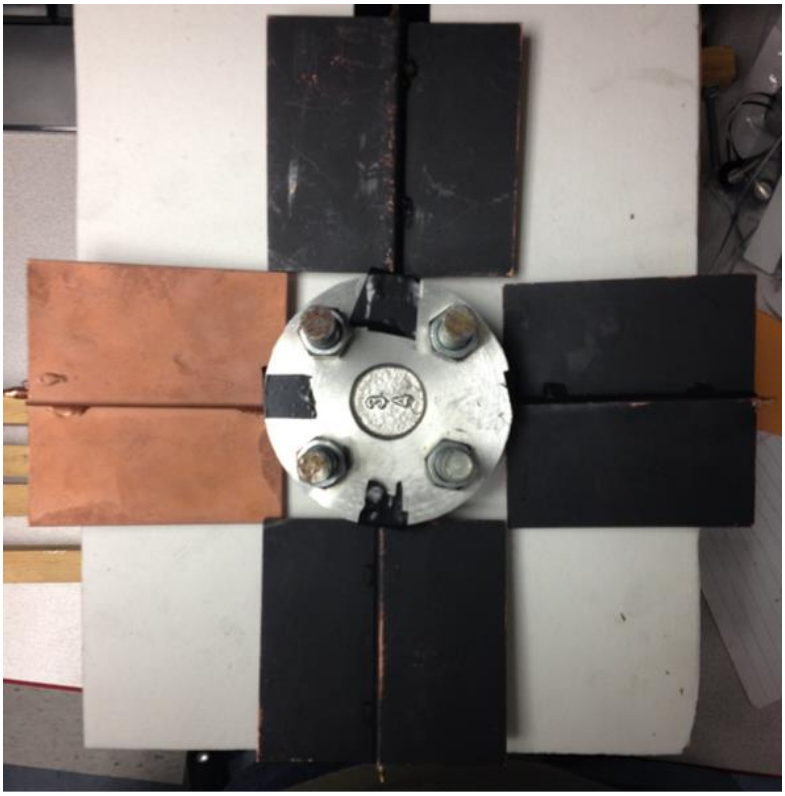

Figure 3-2 View of Bottom of Device with Fins Perpendicular to Device

In order to ensure an as uniform as possible heat distribution, small copper rod inserts were cut and placed around the hot heat exchanger and were in contact with the heat pipes. This was done so that heat from the heat pipes would flow directly into the hot heat exchanger at that contact point as well as to the neighboring copper pieces so that the heat could be applied at multiple points around the heat exchanger. The copper rod inserts had a diameter of 5 mm, the same diameter s the heat pipes, and were 12.7 mm long so that they were in full contact with the heat exchanger. In order to keep the copper inserts and the heat pipes together without damaging the heat pipes, a 3 mm rubber strip was placed around them and then a hose clamp was used to secure everything to the device. Figure 3-3 shows the tip of the heat pipe, the copper inserts that circle the heat exchanger, the rubber strip that encircles everything, and the hose clamp that holds everything together. Figure 3-3 shows that there are six heat pipes because two additional fins were created later.

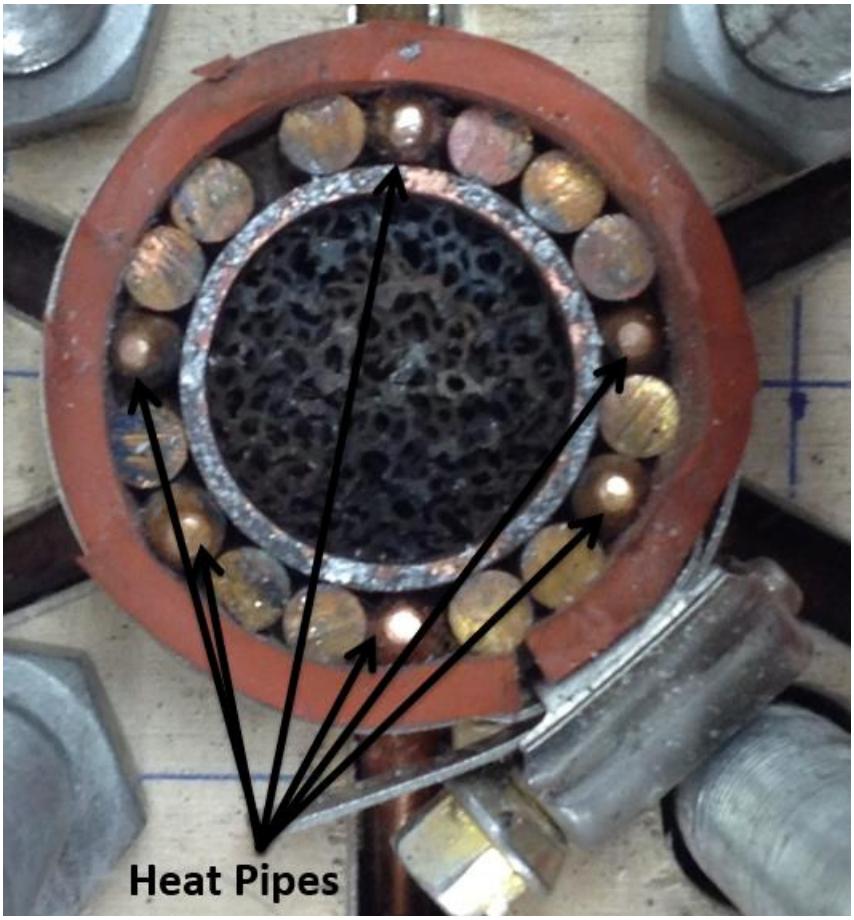

Figure 3-3 Configuration of Heat Pipes, Copper Rod Inserts, and Rubber Strip

Besides the different mode of applying heat to the device, one of the major differences with the radiant panel tests is that the radiant panel will apply heat to the entire device if it can "see" it. A problem arises if any part of the device besides the hot heat exchanger or MACOR end cap receives heat because the rest of the device is supposed to be kept cool. A barrier was created from plywood and insulation that prevented the radiation from the panel from reaching the rest of the device. Figures 3-3 and 3-4 show the barriers used for testing with four fins and six fins, respectively. The device would be assembled by first setting down the MACOR end cap. The barrier would then be slid down the threaded rods and just past the end cap. The barrier would be held in place by nuts on the rods. The rest of the device would then be assembled on MACOR end cap, including the hot heat exchanger with the copper inserts already in place around it. The fin/heat pipe collectors would be added after the device was secured by slipping the heat

pipes through the slits in the barrier and into the spaces left around the hot heat exchanger. Once in place, the hose clamp was securely tightened.

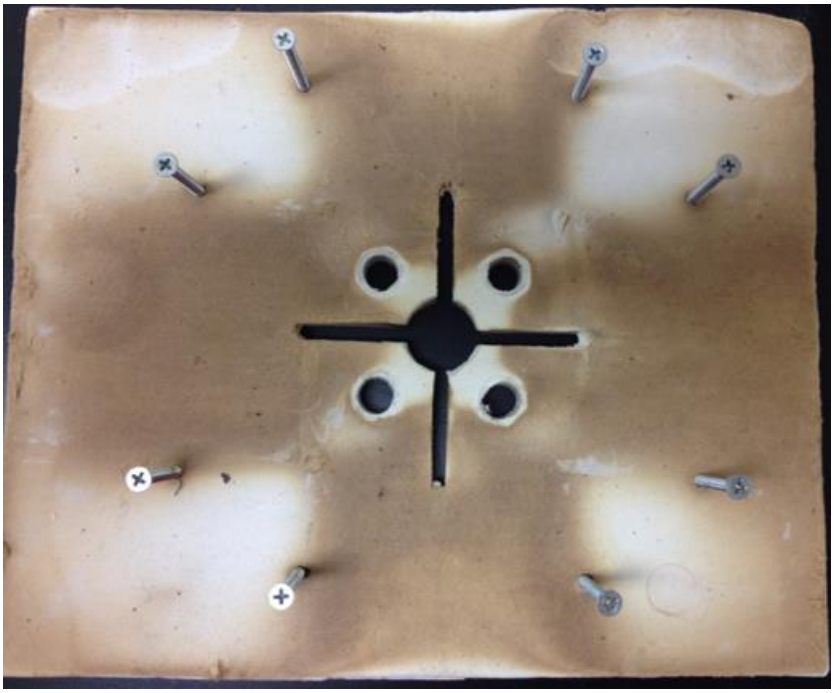

Figure 3-4 Barrier for 4 Fin Configuration

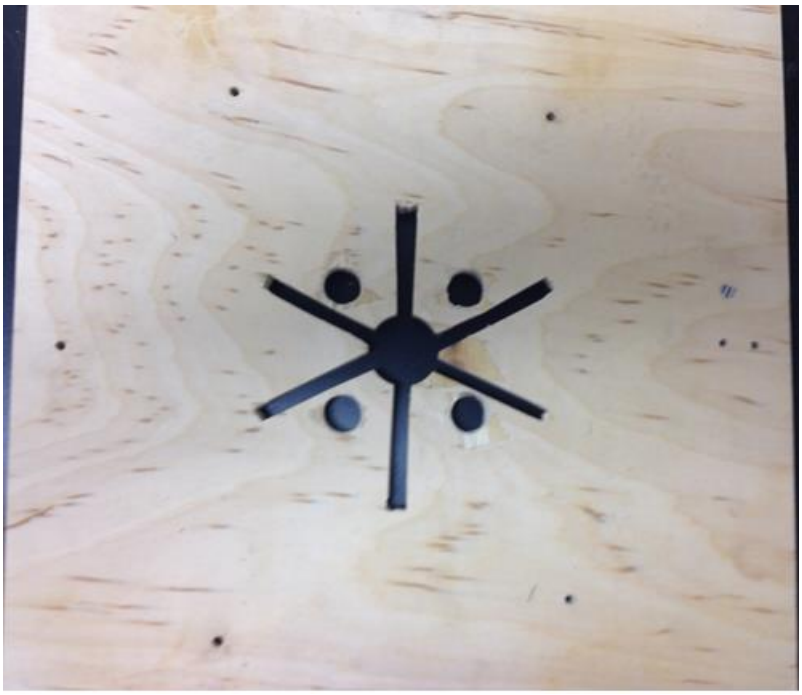

Figure 3-5 Barrier for 6 Fin Configuration

The radiant panel tests were conducted using a vertical gas panel measuring 30.5 cm wide and 45.1 cm tall. The panel burned propane which was delivered at a rate of approximately 1 m^3/hr. Due to the orientation of the panel, the device was required to be held horizontally which is different from the orientation used during the band heater tests. For these experiments, it was desired to expose the device to the same heat fluxes that are consistent with flashover. In order to do this, the heat flux was measured at different distances from the panel in order to find a distance that corresponded to 20-25 kW/m^2. Figure 3-6 shows how the device was positioned during testing using the radiant panel. Because the device is horizontal instead of vertical, the cold heat exchanger could not be cooled exactly as it was during the band heater tests. Instead, an ice cube was manually held in place on the cold heat exchanger. The temperature of the hot heat exchanger was measured on the outside of the heat exchanger between a heat pipe and a copper insert using the same Type K thermocouple probe that was used in the electric band heater tests.

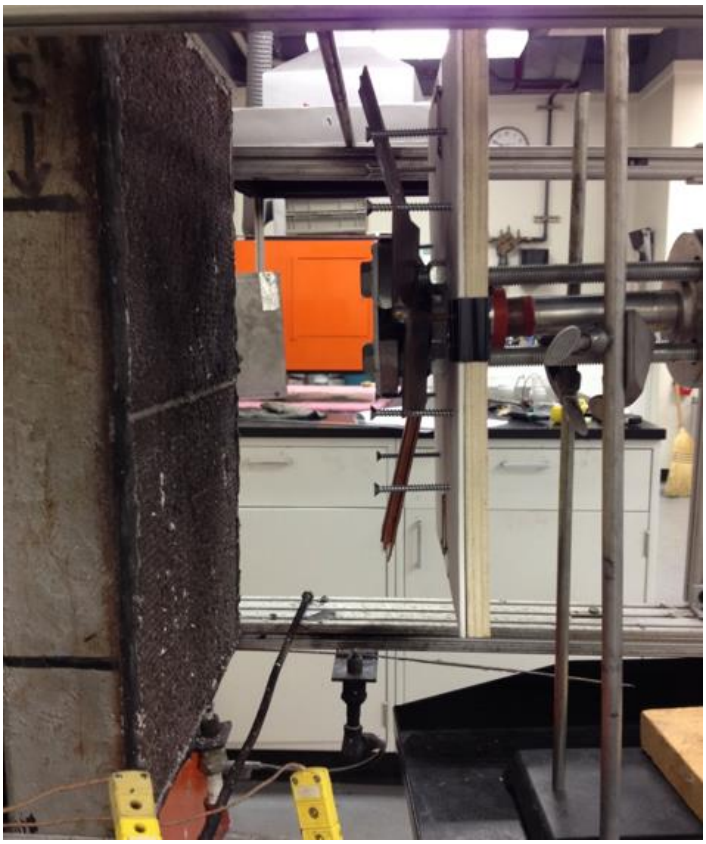

Figure 3-6 Positioning of Thermoacoustic Flashover Detector during Radiant Panel Tests

The initial round of radiant panel testing used the same setup that was found to work best for the electric band heater; the stack was made from rolled steel wool to a mass of approximately 0.70 g and approximately 0.3 mL of water was added to the stack. Under these test conditions and using four fins, the hot heat exchanger was observed to reach temperatures between 170-200°C but activation of the device did not occur after 20 minutes. During this series of tests, it was observed that it was possible to hear the water inside of the device boiling.

In order to maximize the heat transfer to the hot heat exchanger from the heat pipes, a 1.27 cm thick strip of flexible insulation was wrapped around the rubber strip and hose clamp. Figure 3-7 shows the insulation wrapped around the hot heat exchanger as well as the ice cube placed over the cold heat exchanger. Based on the boiling sounds heard in the first set of tests, it was hypothesized that due to the much longer heating time, the water vapor had enough time to escape the stack and the cold heat exchanger before the device activated. Therefore, more water was added to the stack in order to ensure that there would still be water in the stack when the device reaches its activation temperature.

3.3 Results and Conclusions

With this modified setup, the device activated at 125°C after 7 minutes under an exposure of 24 ± 2 kW/m^2. With this same setup, the device activated at 116°C after 8 minutes under an exposure of 22 ± 3 kW/m^2 and 140°C after 19 minutes under and exposure of 19 ± 2 kW/m^2. For each of these tests, approximately 1.5 mL of water was added to the stack. Table 3-1 shows these results for the tests using four fin/heat collectors. These tests show that it is possible to activate a thermoacoustic device by absorbing radiant heat and transferring it to the device via fins and heat pipes. At the time of writing, this is the first instance that a thermoacoustic device has activated using unconcentrated radiant heat.

Figure 3-7 Insulation and Ice Cooling for Thermoacoustic Device during Radiant Panel Tests

Table 3-1 Device Characteristics for Activation Using Radiant Panel and 4 Fins

Stack Mass (g)	**Heat Flux (kW/m^2)**	**Onset Temperature (°C)**	**Activation Time (min)**
0.72	24 ± 2	125	7
0.70	22 ± 3	116	8
0.70	19 ± 2	140	19

Once the device was made to work, it was desired to have the device activate faster in order to provide firefighters with more advanced warning of impending flashover. In order to achieve this, it was necessary to increase the heat transferred to the device. This was accomplished by increasing the number of fins attached to the device to six. The increase in number of fins greatly improved the activation of the device; the device activated at 125°C after 5.5 minutes under an exposure of 25 ± 1 kW/m^2. This design change, however, had the same faults as the four-fin design and electric band heater in that it had to be

constructed to prevent any air leaks. It became hard to ensure air tightness by the joints on either side of the hot heat exchanger due to the copper inserts and rubber strip.

Figures 3-8 through 3-10 show the temperature evolution of the hot and cold heat exchangers during radiant panel tests under exposures of 24 ± 1 kW/m^2. While the temperatures of the cold heat exchanger vary significantly from test to test, the hot heat exchanger temperature increases consistently between tests which confirms that the fins and heat pipes adequately absorb radiant heat and transfer it to the device. The cold heat exchanger temperature varies due to the fact that an ice cube had to be held in place. This allowed for the ice cube to move slightly and potentially cool either the stack holder or the resonator tube in addition to the cold heat exchanger. This variation in cooling as well as differences in ice cube size between tests alters how long it takes for the ice cube to melt, which in turn varies the temperature of the heat exchanger. Another difficult thing to control was the location that was being measured by the thermocouple probe. It was very hard to secure the thermocouple probe in one location because it was measuring the inside of the cold heat exchanger whereas the exterior of the hot heat exchanger was measured. Probe movement might account for why the cold heat exchanger data in Figure 3-9 varies greatly. Using this method of cooling, however, yields a seemingly steady state peak temperature of approximately 120°C, as seen towards the second half of the tests in Figures 3-8 and 3-10.

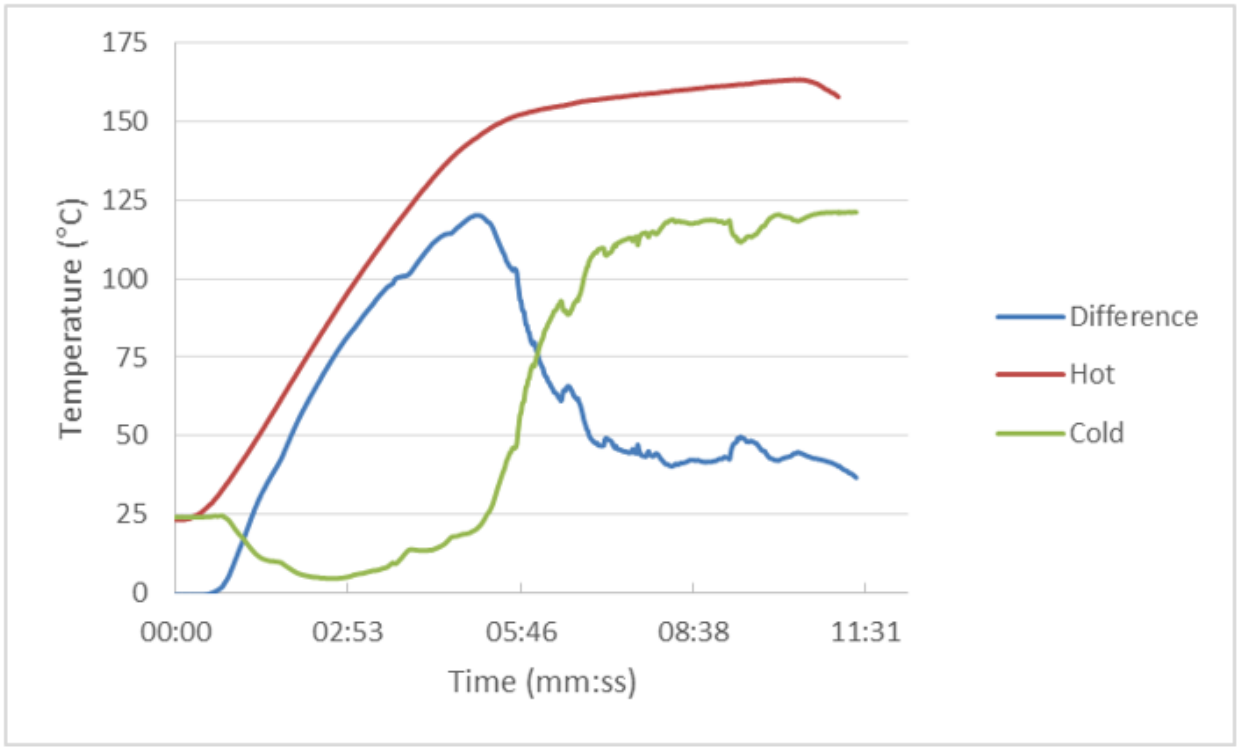

Figure 3-8 Temperature of Heat Exchangers during Radiant Panel Test under Exposures of 24 ± 1 kW/m^2

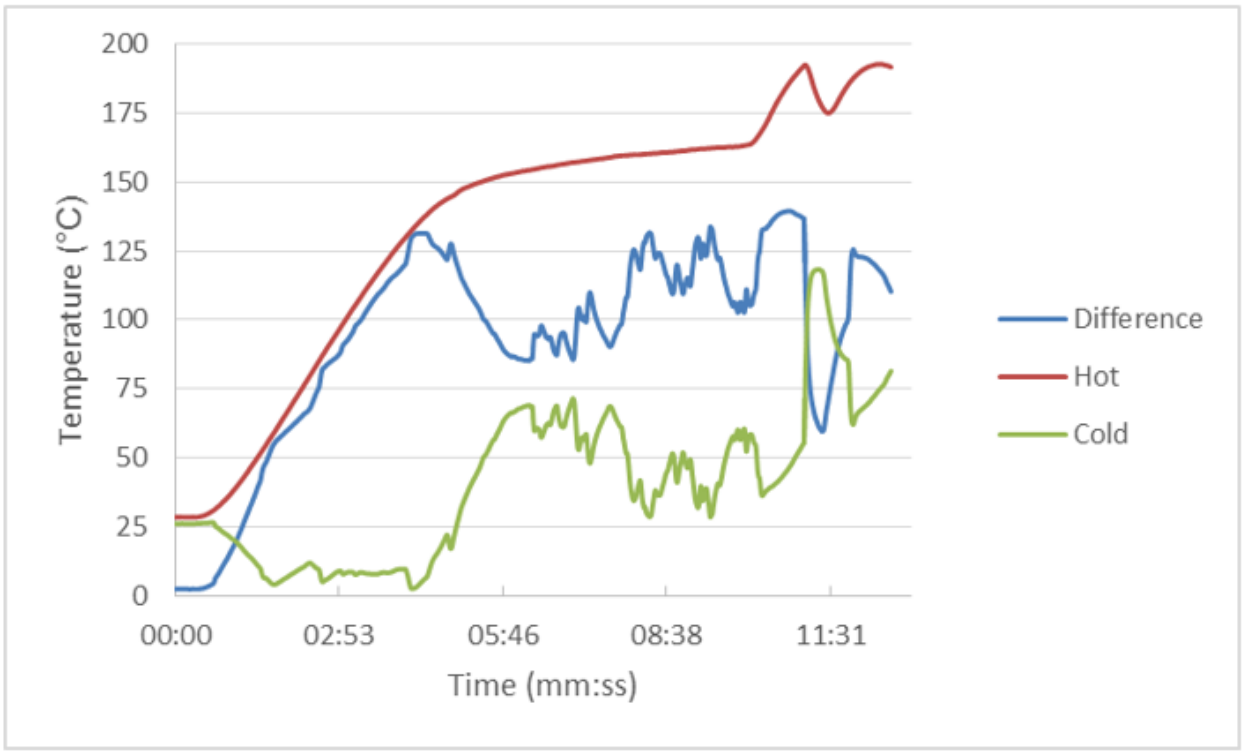

Figure 3-9 Temperature of Heat Exchangers during Radiant Panel Test under Exposures of 24 ± 1 kW/m^2

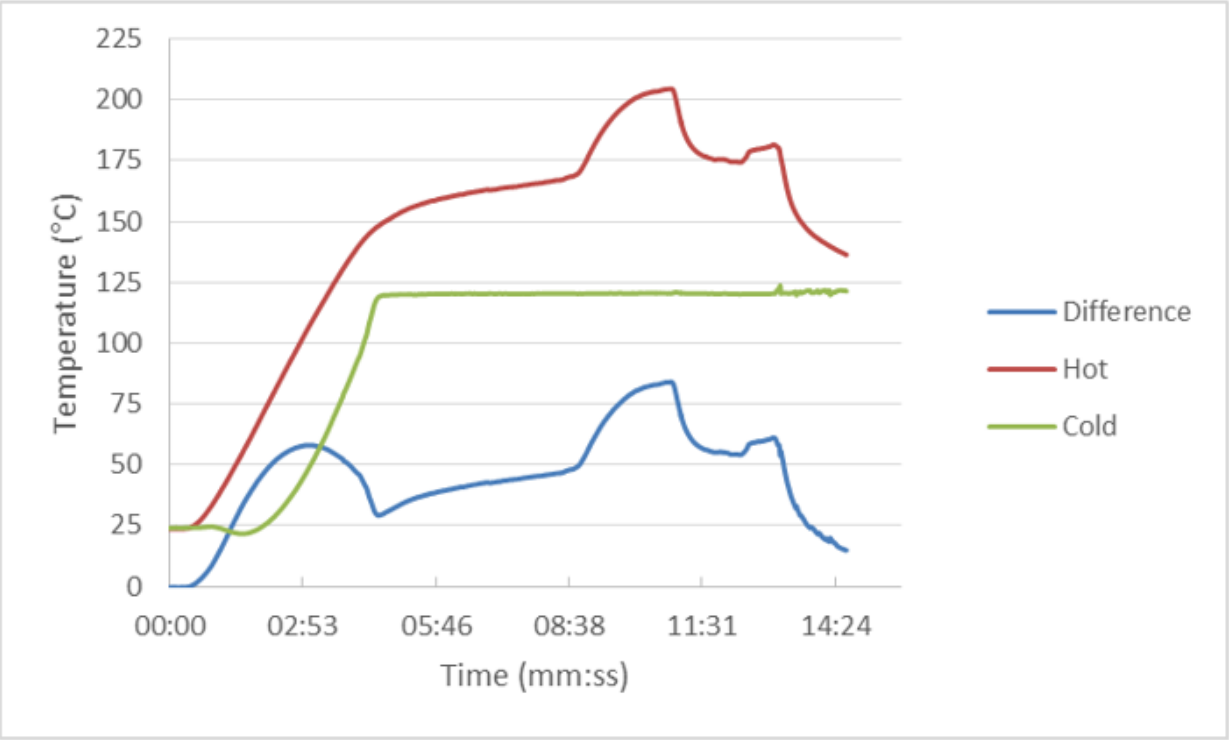

Figure 3-10 Temperature of Heat Exchangers during Radiant Panel Test under Exposures of 24 ± 1 kW/m^2

4 Testing Stage 3: MFRI

4.1 Motivation and Objectives

Once the device was shown to work using radiant heat from a propane panel, it was desired to test the device in a fire environment to determine if it would still work in conditions that firefighters would expect to encounter. There were four stages to this testing: designing housing for the device during testing, designing a new cooling system for the device, characterizing the burn room using thermocouples and a heat flux gauge, and finally testing the device. The full scale testing was conducted in one of the burn rooms at the Maryland Fire and Rescue Institute (MFRI) at the University of Maryland.

4.2 Methods

4.2.1 Device Housing

Due to the fact that this device is simply a prototype and not fully optimized for field testing, it was necessary to provide protective housing for the device so it did not become damaged during the test. This housing was provided by a galvanized steel cube measuring 35.6 cm x 35.6 cm x 35.6 cm protected with insulation and cooled using water cooled radiators. The housing was the Galvanized QBO® Steel Cube from The Container Store; the insulation was very high temperature mineral wool insulation from McMaster-Carr, product number 9328K43, which was 5.08 cm thick with a temperature range from -18-649°C; and the cooling was provided by two Phobya Xtreme 200mm Radiators, Version 2. The three side walls and the top of the box were covered with the insulation; the door was covered with a separate, thinner, more flexible sheets of insulation. The two radiators were positioned in the box such that one radiator was along the back and the other along the left wall, forming a corner. This was done with the intent that that particular corner of the box would be facing the fire. Holes were cut into the bottom of the box in order to supply water to the radiators via a manifold and to allow the water to drain out of the box. A hole was cut into the top of the box so that the device could be lowered into the box while leaving the

fins outside. Figure 4-1 shows the interior of the box with the insulation, radiators, water supply, and the device sticking down into the box.

Figure 4-1 Inside of Device Housing

4.2.2 Cooling System

Unlike the previous two test setups, it is impossible to cool this device due to its orientation and the environment in which the device will be tested. In order to cope with the heat from the fire, a design that utilized flowing water was desired in order to provide consistent cooling to the device. This cooling device was made from two machined pieces of aluminum, measuring 5.08 cm x 5.08 cm, held together by four screws. The bottom piece was made from 2.54 cm thick aluminum which fed by a 0.64 cm water line coming into the bottom of the piece. The water flowed into a 0.33 cm wide, 0.64 deep water channel

though a 0.20 cm hole that connected it to the water line. A 3.18 cm diameter hole was drilled through the length of this piece which allowed for a 3.18 mm gap between the cooling device and the cold heat exchanger. The top piece was made from 3.18 mm thick aluminum with a 2.54 cm hole drilled through the center. The two pieces were separated by a 1.68 mm thick, 4.42 cm ID soft Buna-N O-ring from McMaster-Carr, product number 2418T133. The four screws allowed the top plate to be loosened or tightened to the bottom piece as desired. The thickness of the separation was approximately 0.10 mm. All of this together created a water jet stream that sprayed against the cold heat exchanger in order to cool the device. This cooling device was placed in line with the device so that it would sit just below the stack holder and spray water onto the cold heat exchanger. The gap around the top plate was sealed using a Permatex RTV sealant in order to prevent was from spraying up and cooling the hot heat exchanger as well as to hold the cooling device in place. The water would then run down the resonator tube and provided some additional cooling to the device. Table 4-1 provides some of the dimensions for the bottom piece of the cooling device. Figures 4-2 through 4-7 show various views of the water cooling device and how it attached to the cold heat exchanger.

Table 4-1 Bottom Piece of Cooling Device Component Sizes Starting from the Center

Bottom Piece Component	Size (mm)
Hole Radius	15.88
Wall Thickness	1.02
Water Channel	3.30
Water Channel Depth	6.35
Water Supply Hole	2.03
Wall Thickness	0.51
O-ring Groove	2.54
O-ring Depth	1.27

Figure 4-2 Side View of Resonator Tube with Water Cooling Device

Figure 4-3 Top View of Cooling Device around Cold Heat Exchanger

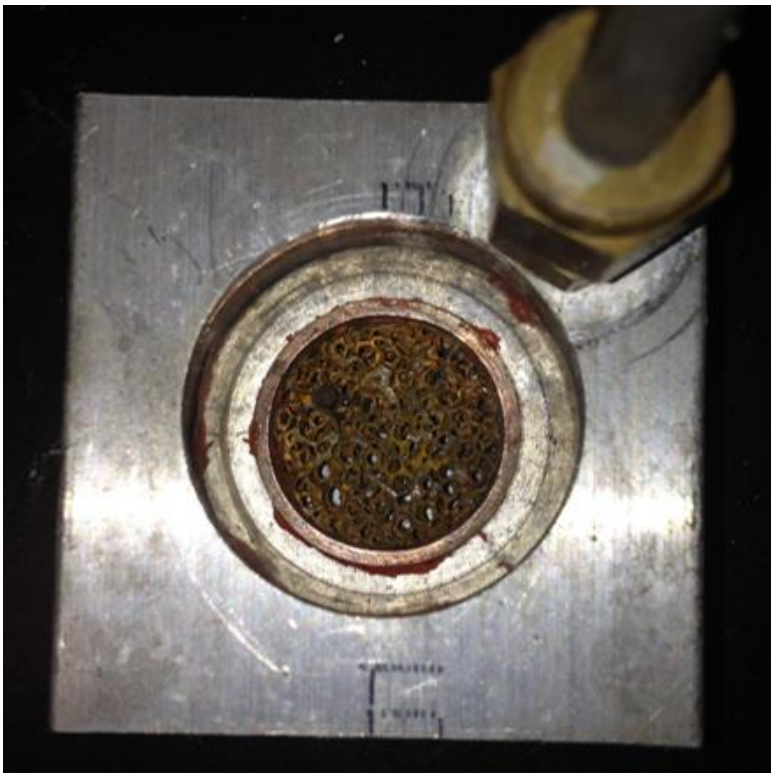

Figure 4-4 Bottom View of Cooling Device around Cold Heat Exchanger

Figure 4-5 Top View of Cooling Device with Pieces Separated

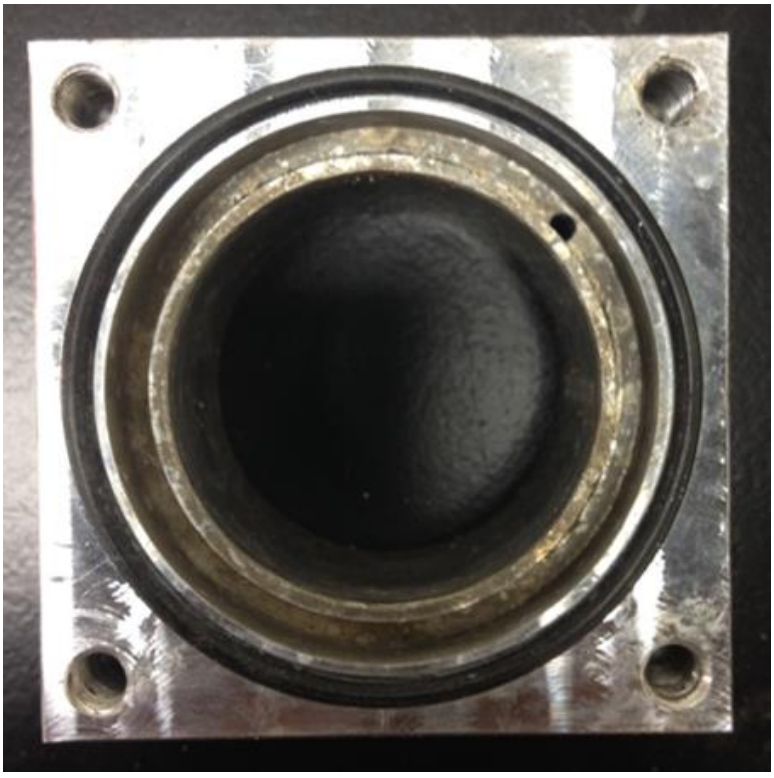

Figure 4-6 Top View of Bottom Piece of Cooling Device Showing O-ring, Water Groove, and Water Supply Hole

Figure 4-7 Bottom View of Bottom Piece of Cooling Device Showing Water Connection and Water Hole

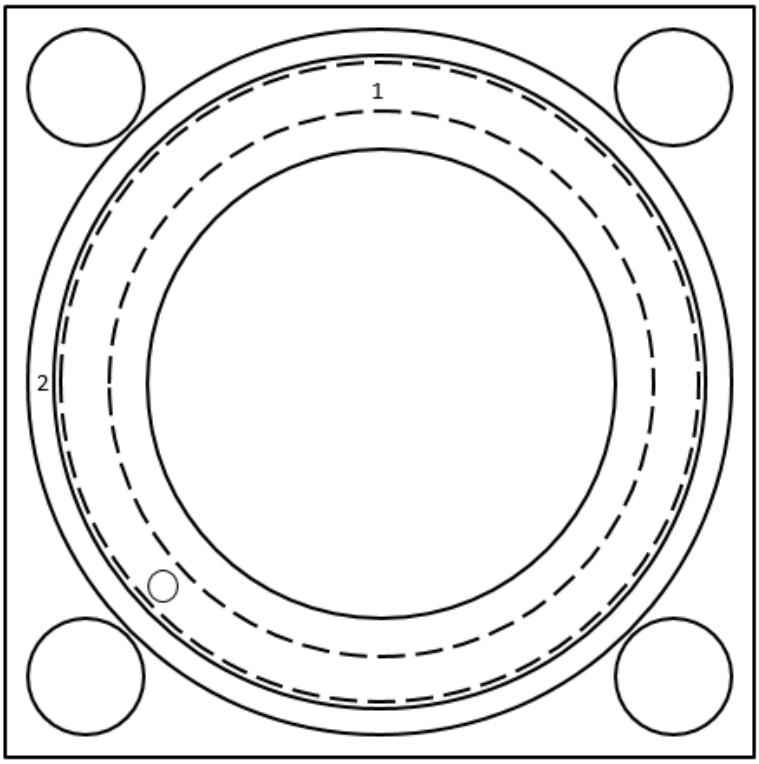

Figure 4-8 Schematic of Top View of Bottom Piece of Cooling Device. The Dashed Ring (1) Represents the Water Groove and the Solid Outer Ring (2) Represents the O-ring. Drawing not to scale.

4.2.3 Fire Environment

The first testing that was done at MFRI was to characterize the burn room that would be used for the tests. The burn room was a concrete room on the third floor of the MFRI burn building measuring 3.1 m x 3.3 m x 2.8 m with openings on the east and west sides of the room. The east opening was 1.2 m wide and went to the ceiling, and the west opening was 0.8 m wide and 2.0 m tall. A square 45 cm x 45 cm beam ran from the north to south side of the room, 86 cm from the west wall [17].

The material used for the fire consisted of wood pallets and wood shavings that were placed on a raised 1.5 m x 1.5 m tray located in the northwest quadrant of the room. Figure 4-9 shows the typical starting amount for each test; more pallets and shavings were added as necessary to extend the length of the tests. Two thermocouple trees were placed in the room, one in the middle along the south wall and the other north of the east opening. Each tree was 2.44 m tall and had eight thermocouples per tree. Table 4-2 shows the heights of the thermocouple used on each tree during these characterization burns. The thermocouples were spaced closer together near the top of the tree in order to obtain a better profile of the smoke layer. A heat flux gauge was also used in the burn room characterization to determine the heat flux that the device would receive from the smoke layer. The heat flux gauge was placed in the box designed to hold the device along with another thermocouple to observe how the temperature inside the box changed during the duration of the test. The box was placed on a steel rack on the north side of the east opening. Between each test, the height of the box was altered in order to find the optimum height to mimic the heat flux exposure used in the radiant panel tests and consistent with flashover. The heat flux gauge was located at 1.47 m, 1.63 m, 1.78 m and 2.03 m during the various tests. Figure 4-10 shows the configuration of the burn room for each of the tests.

Figure 4-9 Standard Burn Configuration

Table 4-2 Height of Thermocouples during Burn Room Characterization

South Tree (m)	East Tree (m)
2.26	2.26
2.08	2.13
1.88	1.98
1.73	1.80
1.30	1.52
1.12	1.30
0.86	1.12
0.76	0.84

Figure 4-10 Burn Room Configuration Looking from the West Wall towards the East Wall

Figures 4-11 through 4-14 show the temperatures measured by the highest four thermocouples from each tree and the measured heat flux for the duration of each test. These figures, especially Figure 4-12, show a strong correlation between smoke layer temperature and heat flux. Using the data from Figure 4-12, it was possible to derive a correlation for the measured heat flux based on the thermocouple measurements on the East Tree:

$$HF = 0.057T - 4$$

where T is the temperature at the top of the thermocouple tree measured in °C and HF is the heat flux from the smoke layer measured in kW/m^2. Based on this correlation and the observed temperatures and heat fluxes from the characterization tests, achieving a heat flux of 24 kW/m^2, which was the imposed heat flux during the radiant panel tests, requires a smoke layer temperature of approximately 500°C.

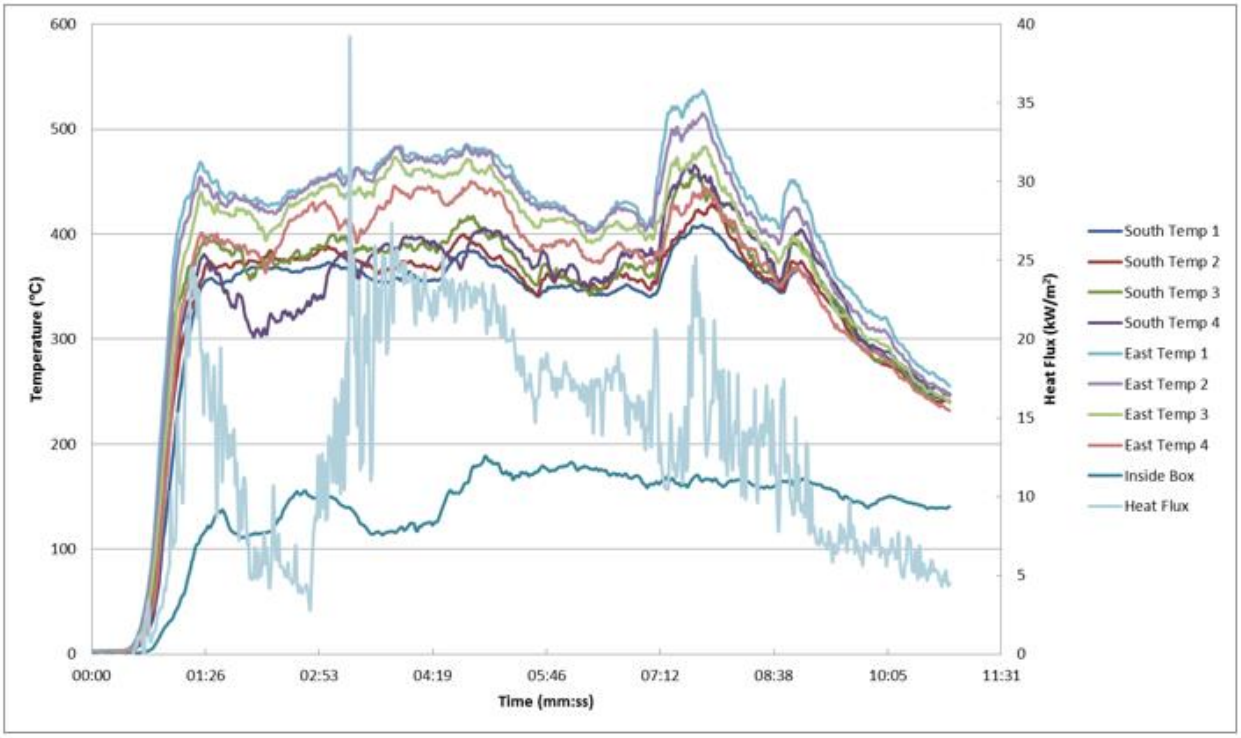

Figure 4-11 Top 4 Thermocouples and Heat Flux vs Time with the Heat Flux Gauge Positioned at 1.47 m

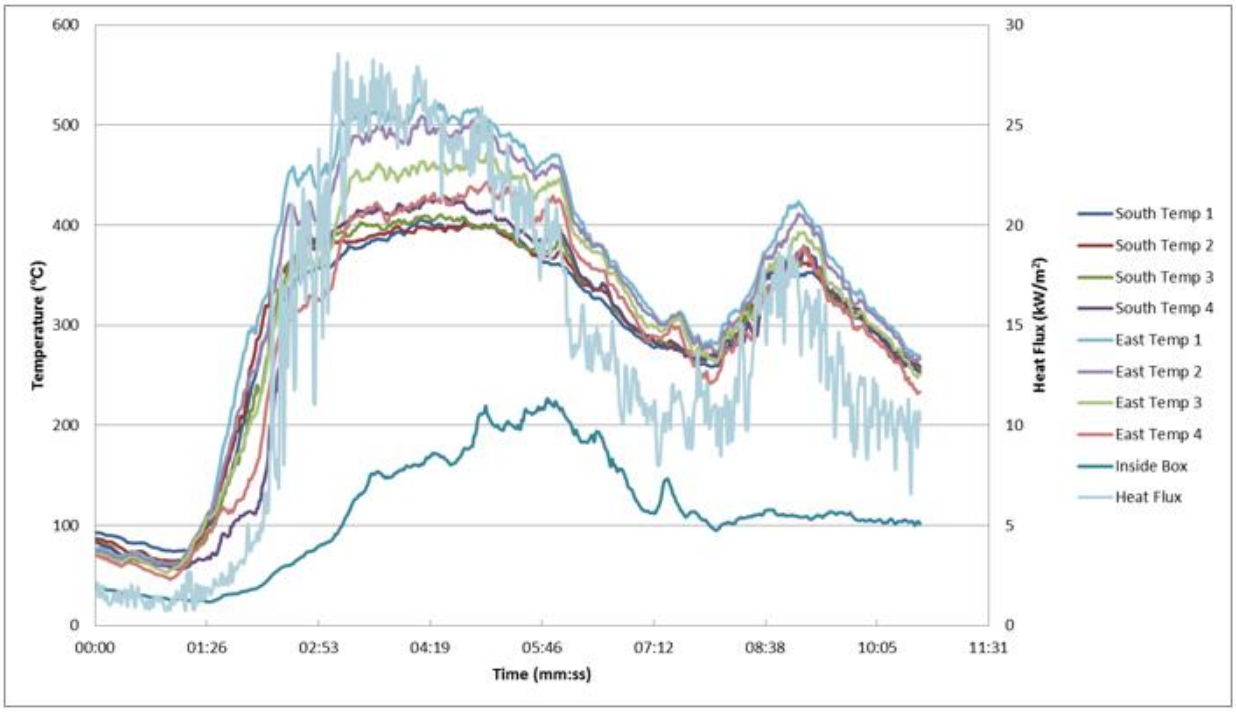

Figure 4-12 Top 4 Thermocouples and Heat Flux vs Time with the Heat Flux Gauge Positioned at 1.63 m

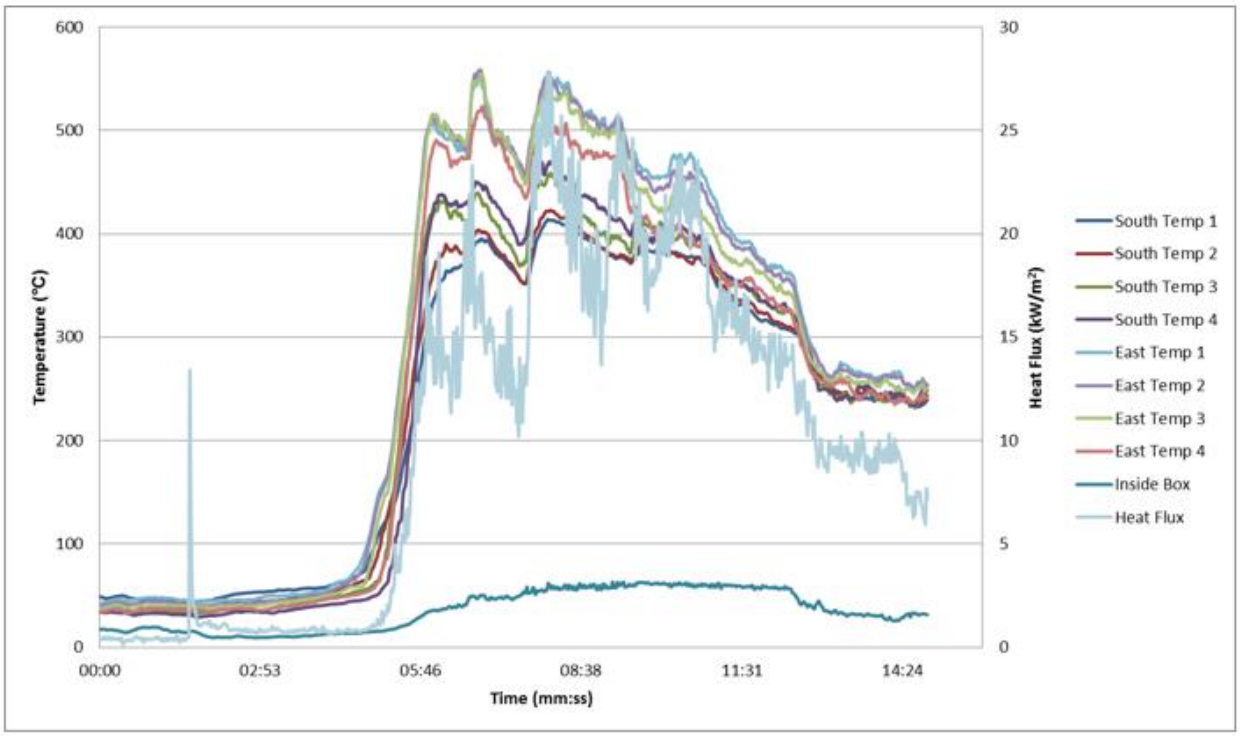

Figure 4-13 Top 4 Thermocouples and Heat Flux vs Time with the Heat Flux Gauge Positioned at 1.78 m

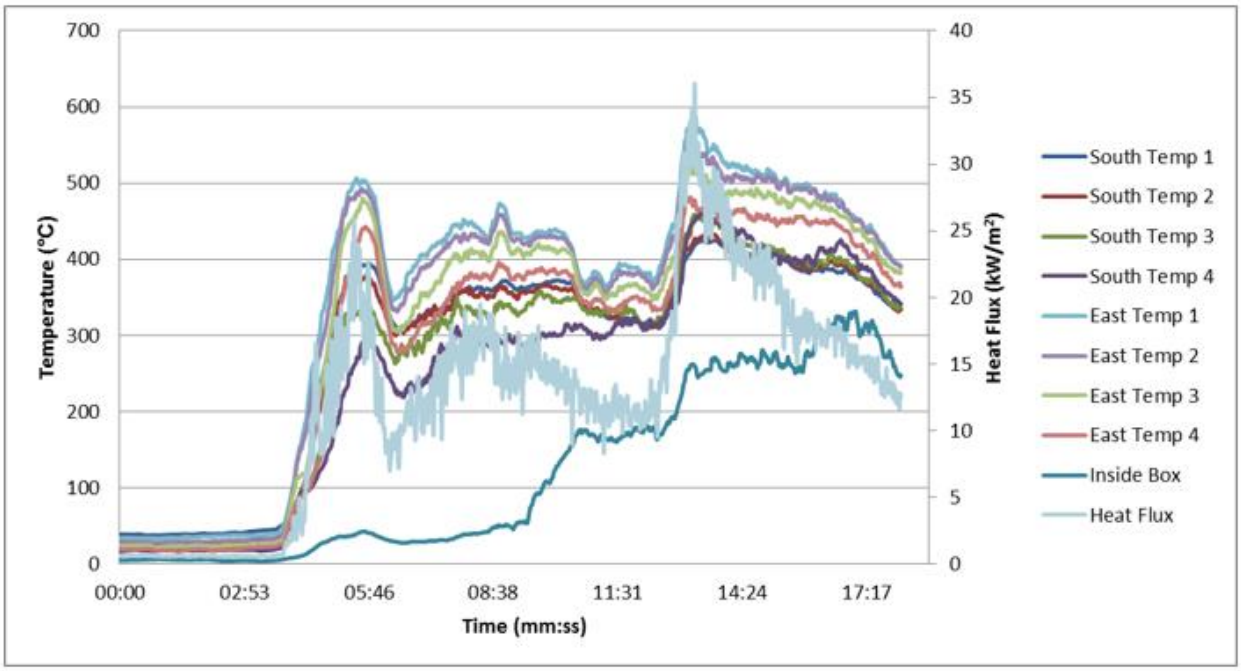

Figure 4-14 Top 4 Thermocouples and Heat Flux vs Time with the Heat Flux Gauge Positioned at 2.03 m

4.2.4 Fire Testing

For the actual fire tests with the device at MFRI, the box containing the device was positioned on the rack such that the fins were located approximately 1.90 m above the floor. This height was chosen in

order to simulate the actual height of the top of a firefighter helmet and ensure that the fins received as much radiation as possible. Based on the results of the room characterization, it was desired to sustain a temperature of 500°C for at least 6 minutes in order to provide the same heat flux as the radiant panel for the lowest observed activation time during the radiant panel tests. This was done by monitoring the real-time thermocouple measurements during the tests and adding more pallets and wood shavings as necessary. For these tests, a different set of measurements from the characterization tests were recorded. The two thermocouple trees remained in the same place. Besides measuring the temperature in the compartment, they were used to estimate the heat flux based on the correlation derived from the data collected during the room characterization test series. The heat flux gauge was removed from the experiment setup due to lack of space in the box. Two thermocouples were placed inside the box, one to measure the exterior of the hot heat exchanger and one to measure the interior of the cold heat exchanger. There was no thermocouple to measure the interior box temperature. A microphone was also included in the design in order to record whether or not the device activates. The microphone was necessary because no one was allowed in the burn room during the tests besides the MFRI staff to add more fuel. The microphone chosen for this was the Waterproof Pre-Amplified Microphone from Super Circuits due to its size and that it was waterproof. The waterproof feature was necessary for the microphone because there was a chance that water from the cooling device would drip onto the device and potentially damage it. Figure 4-15 shows the interior of the box configured with the instrumentation. The microphone was wrapped around the water line to one of the radiators with its cable connections wrapped in insulation aluminum foil. The thermocouple inside of the device was secured to one of the threaded rods using aluminum tape to ensure that the thermocouple bead didn’t lose contact with the heat exchanger inside the device.

Figure 4-15 Box Interior with Instrumentation

4.3 Results and Conclusions

The full scale tests at MFRI were done in two separate phases that were one month apart in order to allow for time to make any changes to the device. For the first phase of testing, the burn room temperature was held as close to or above 500°C for 10-15 minutes. Unfortunately, various problems arose during testing. The hot heat exchanger connection became loose during testing which corrupted the data. In addition, the microphone wire was exposed to too much heat and began to melt to a point where the signal was unusable. However, the temperature data from the room suggested that the heat flux imposed on the device was equal to or greater than that imposed during the radiant panel tests in the lab. Figure 4-16 shows a sample of the data from one of the tests during the first phase including the correlated heat flux from the smoke layer.

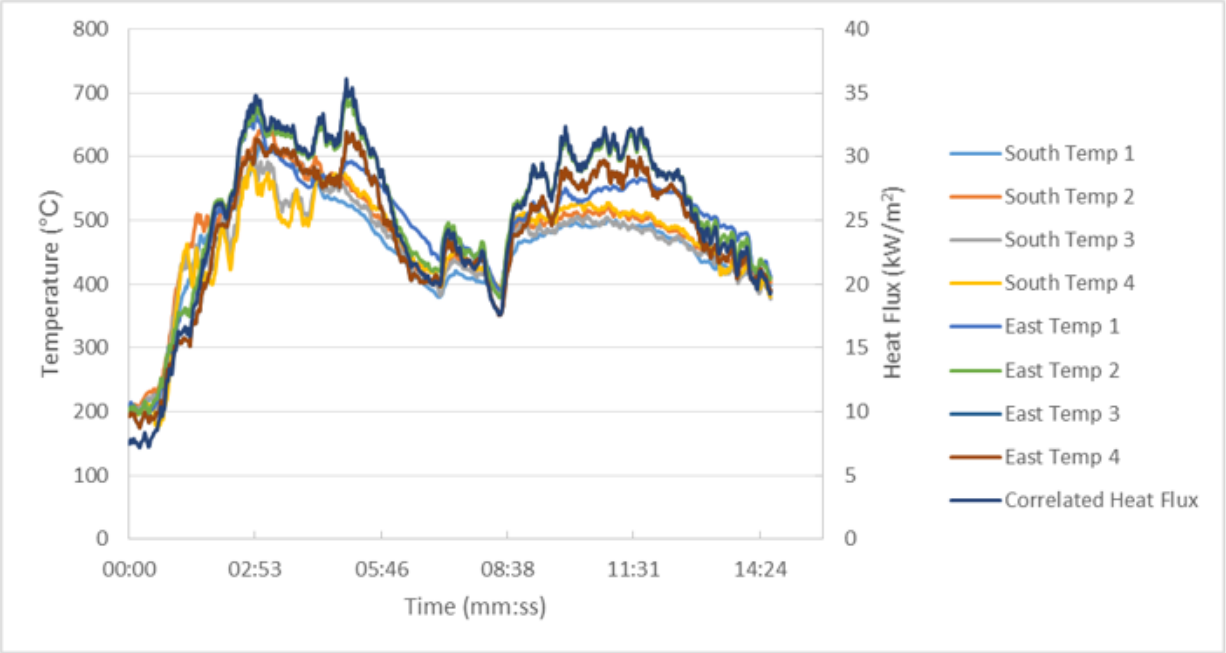

Figure 4-16 First Phase Temperature and Correlated Heat Flux Data

After this round of testing, the MFRI staff noticed some spalling in the north wall. Due to this, MFRI required that the tests go no higher than the temperature requirements that were believed to be sufficient for activation. Therefore, the temperatures for the remaining tests were much closer to 500°C or below with very few times when it becomes hotter than that. In order to compensate for the lower imposed heat fluxes to the device, some of the tests were run for longer in order to give the device more time to heat up. This second round of testing was conducted over the course of two weeks in order to provide time to make any final or more permanent changes to the device before the grant was over. While there were no flaws during the first week of testing, there was no evidence of the device activating. Figure 4-17 shows the top four thermocouple temperatures for each tree, the correlated heat flux based on these temperatures, and the temperatures of the heat exchangers of the device from one of the tests during this first week of testing during phrase two. As the shown in the figure, the temperature of the heat exchangers is very similar to the temperatures that were measured at activation during the radiant panel tests, which suggest that the device should have activated.

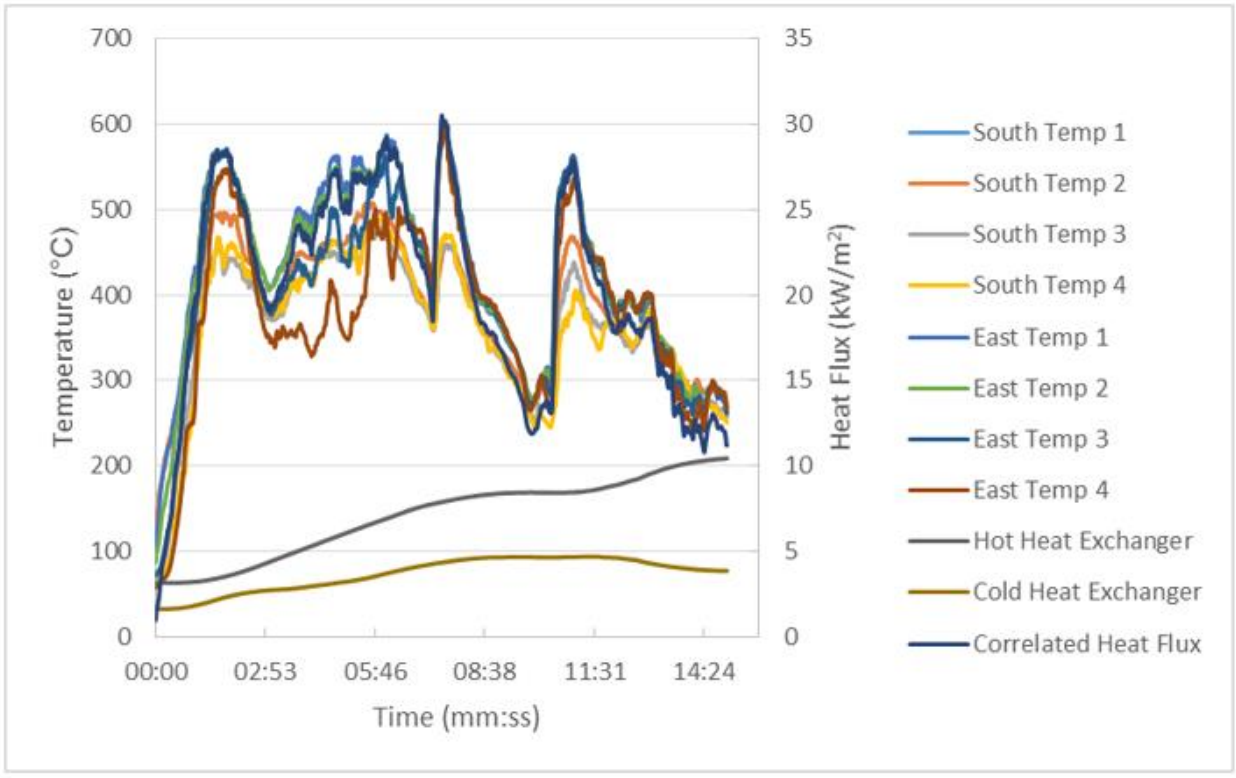

Figure 4-17 Second Phase Temperature, Correlated Heat Flux, and Heat Exchanger Temperature Data

Because the conditions that were present during activation using the radiant panel were achieved during the previous tests, it was believed that the potential cause of failure was that there was a small air gap in the device which would prevent it from working. In order to eliminate as many possible points of leakage, all of the joints of the device except for the joint between the stack holder and the cold heat exchanger were either sealed or resealed using an RTV sealant. During the first two tests of this last week of testing, the cold heat exchanger did not appear to be cooling down as much as it had previously. Once the second test was concluded, the burn room was cooled down in order for the device to be examined. It was found that the water cooling device was not supplying more than trickle of water instead of the jet that it was supposed to deliver. After trying to loosen the screws on top of the device to make the gap larger did not work, increasing the flow to the device was attempted in case some of the RTV sealant had gotten into the gap. Once the flow was increased, the cooling device started properly working. The flow was difficult to maintain between the different stages of testing because it was controlled by a valve that drew water from the fire hose used by the fire fighters. The valve was opened just enough to provide a

steady stream to the device, so it was possible that the change in room conditions between the start and end of the test could have affected the cooling device such that water wasn't getting through the gap between the top and bottom piece of the cooling device. Figures 4-18 and 4-19 show some of the data collected during this second phase of testing. These figures show similar data as in the first phase of testing, but the microphone did not pick up any sound to suggest that the device had activated. Once this final series of testing was over, the device was taken apart and the lip stack holder was found to be broken, however, it is unknown when it broke. It is possible that the stack holder broke while attempting to fix the cooling device. Due to the design of the device, it was impossible to tell if the stack holder was broken during testing because the lip of the stack holder sits in the cold heat exchanger. Based on the results of the first and second phase of testing it is unsure whether the device failed to activate due to leaks in the device or if the temperature requirements for activation are different due to the change in orientation of the device.

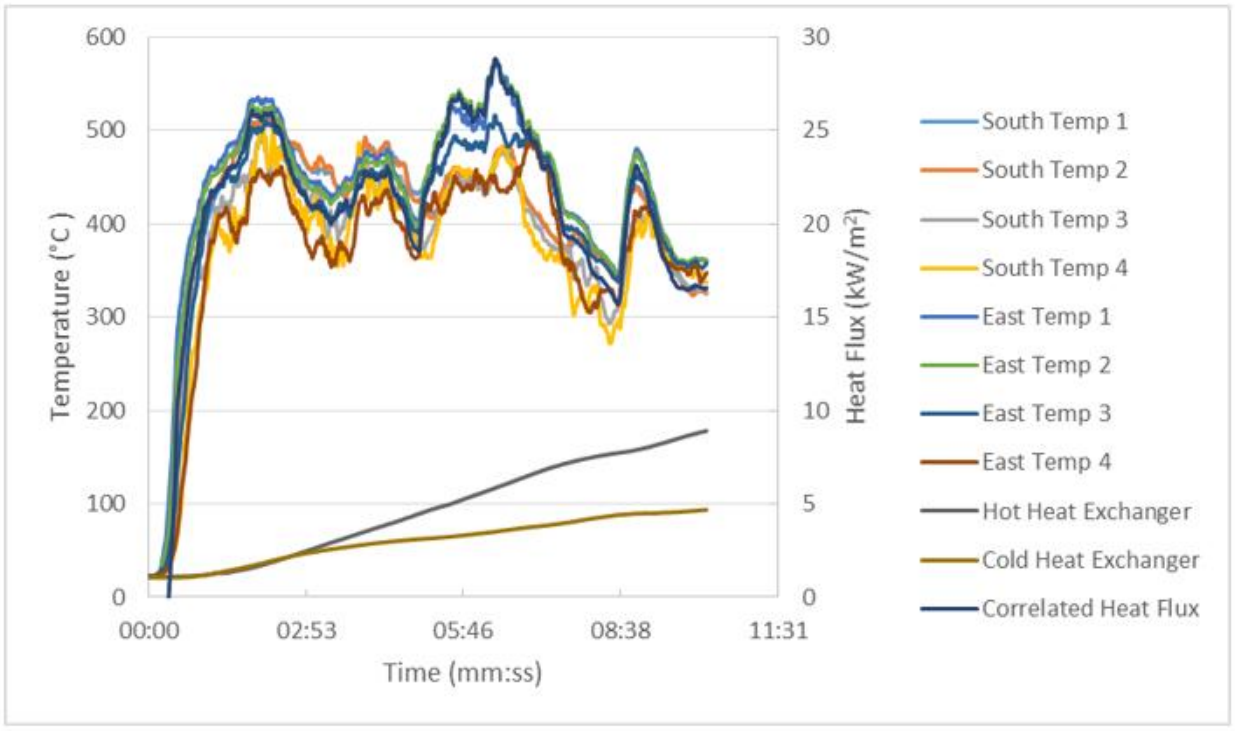

Figure 4-18 Second Phase Temperature, Correlated Heat Flux, and Heat Exchanger Temperature Data

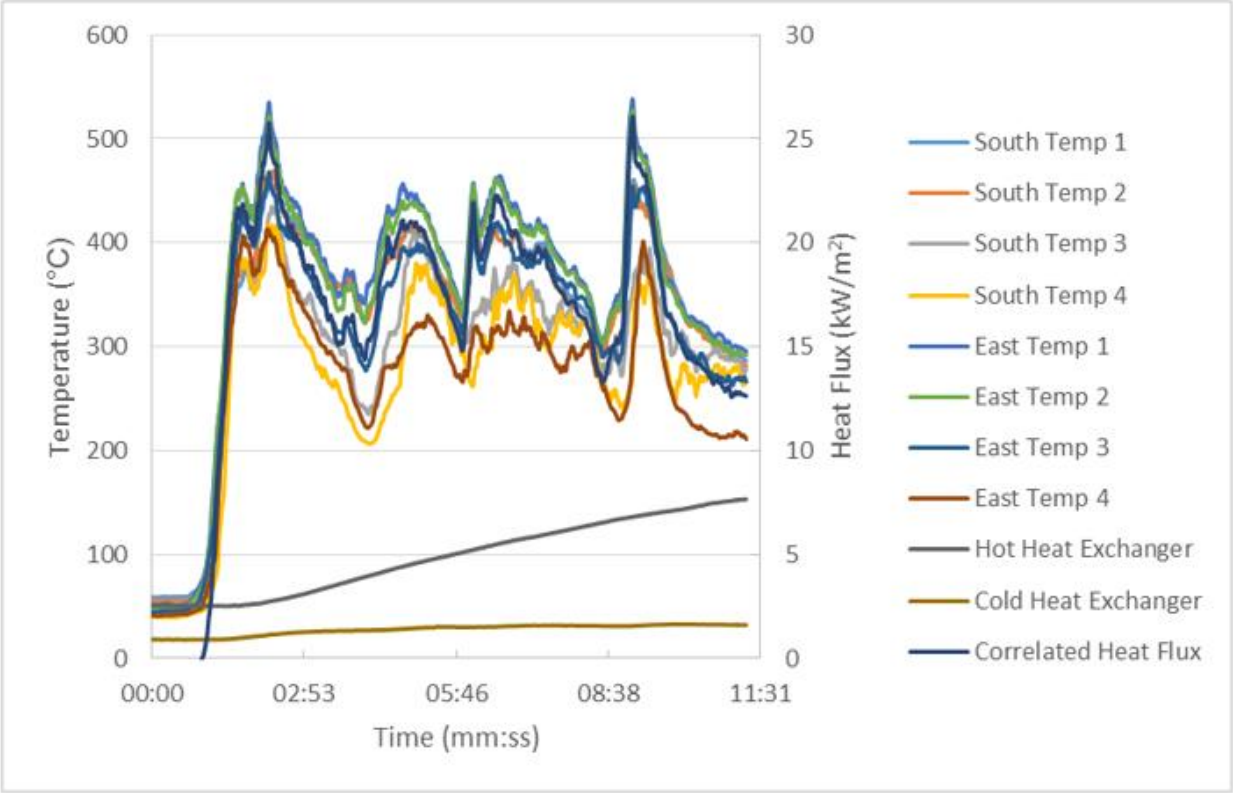

Figure 4-19 Second Phase Temperature, Correlated Heat Flux, and Heat Exchanger Temperature Data

Another possible explanation for the device's failure to activate may be due to the water that was added to the stack. As explained previously, the addition of water acts as a catalyst for the expansion and rarefaction of the gas inside the stack. In vertical orientation used during testing with the electric band heater and the horizontal orientation used during the radiant panel tests, the water vapor would condense on the cold heat exchanger and move back into the stack where it would evaporate again. However, it is possible that in the inverted orientation used in the full scale tests, the water vapor would rise towards the hot heat exchanger and Macor end cap instead of the cold heat exchanger thereby cooling the hot end of the device. Because the device requires a single temperature gradient, it is possible that this additional temperature gradient prevent the device from operating.

5 Conclusions and Suggestions for Future Work

There were many breakthroughs throughout this project based on the original prototype device. When using the electric band heater, the optimum parameters were found to be using a steel wool stack with a mass of approximately 0.70 grams, or a density of 170 kg/m^3, and the addition of approximately 0.3 mL of water to the stack. These parameters consistently yielded activation temperatures of approximately 125°C. Additionally, a critical temperature difference of 30°C was attained with a power input of 8 W. Once this activation temperature was achieved, it was possible to incorporate the copper fin/heat collectors designed by Hamburger into the device and test it using radiant heat instead of using an electric band heater. This design change proved challenging but the device was still able to activate using four copper fin/heat collectors, adding 1.5 mL of water, under an exposure to a heat flux of approximately 24 kW/m^2 for approximately 7 minutes with an activation temperature of 125°C. The addition of two more copper fin/heat collectors increased the time to activation under the same heat flux exposure. This was the first time that a thermoacoustic device has activated due to unconcentrated radiant heat. After it was shown that it was possible for the device to activate radiant heat, full scale fire tests were conducted at a burn room at MFRI in order to see if the device would work in a real fire scenario as opposed lab conditions. After a few rounds of testing, the device did not activate. Based on the data collected, it is unsure if the device did not activate due to leakage in the device or if the temperature requirements for activation are different due to the change in orientation of the device because the device reached similar temperatures on the hot and cold heat exchangers.

If this project were to continue, potential future work would be looking into the different conditions required for activation with the device held in different orientations. The work could start with testing the device using the band heater at different power inputs to determine the minimum activation requirements in the horizontal and inverted positions. Due to the design of the device, the device would most likely need to be in the horizontal or inverted position in order for the fins to be positioned closer to the smoke layer to receive as much radiation as possible. Once the minimum activation conditions were determined,

it would be necessary to compare the activation conditions for activation using radiant heat. During this research, it was only possible to test the device using a vertical radiant panel. A setup would need to be devised in order to test the device in the inverted position using a radiant panel as well. If the heat flux and temperature requirements are greater in the vertical position than the horizontal, a potential design change could be to keep the device horizontal but reconfigure the copper fin/heat collectors to be facing the ceiling in order to absorb the maximum amount of radiation.

While readjusting the copper fin/heat collectors might improve the performance of the device by reducing the necessary critical temperature difference and power requirements for activation, changing the heat pipe itself could have an impact as well. It is possible that while the temperature gradient that was observed during the radiant panel tests was attained during the full scale testing at MFRI, the heat transfer from the heat pipes was not as efficient as it could have been due to the working fluid in the heat pipe being water. For heat pipes to be efficient, it is necessary for the working fluid to undergo phase transitions; due to the environment in which the heat pipe is exposed, it is possible that the cool end of the heat pipe became too hot for the water to condense and thereby slowed down the heat transfer process. It is also possible that during the full scale testing, when the device was inverted, that the buoyancy of the water vapor overcame the effect of gravity which prevented the vapor from reaching the cool end of the pipe.

Another design enhancement to make is permanently connect the various pieces of the device in order to minimize the chances of leaks as well as enhancing the durability of the device. Two options for this would be using a more permanent sealant or having the device constructed so that it is all one or two pieces that fit together and form an airtight seal. Creating the device out of solid pieces instead of using a sealant would be more ideal, however, because sealant can break. Finding a replacement material for Macor would also be advised due to its fragility. As seen in the final tests at MFRI, the Macor stack holder had broken which is the most likely cause of failure during that round of testing. The final change would be to find a way to keep the stack permanently wet or change the stack material so that water is not required in the final detector in order to reduce the complexity of the device from a construction and

reliability standpoint. As mentioned in Section 2.3, it might be worthwhile to try and optimize the device to work with fine bronze wool or test other stack materials. Testing other materials would ensure that the lowest temperature requirements are necessary to activate the device.

6 References

[1] Karter, Jr., Michael, and Joseph Molis. “US Firefighter Injuries – 2012.” National Fire Protection Association, 2013.

[2] Fahy, Rita, Paul LeBlanc, and Joseph Molis. “Firefighter Fatalities in the United States – 2012.” National Fire Protection Association, 2013.

[3] ISO. “Glossary of Fire Terms and Definitions,” ISO/CD 13943, International Standards Organization, Geneva, 1996.

[4] Karlsson, Björn, and James Quintiere. *Enclosure Fire Dynamics*. CRC Press, 2000.

[5] Mensch, Amy, George Braga, and Nelson Bryner. “Fire Exposures of Fire Fighter Self-Contained Breathing Apparatus Facepiece Lenses.” National Institute of Standards and Technology, 2011.

[6] Newman, Jonathan, Bob Cariste, Alejandro Queiruga, Isaac Davis, Ben Plotnick, Michael Gordon, and Sidney San Martin. “Thermoacoustic Refrigeration.” GSET Research Journal, 2006.

[7] Hamburger, Kenneth. “Optimization and Implementation of a Thermoacoustic Flashover Detector.” *Master’s Thesis*, 2013.

[8] Jung, S. and K. Matveev. “Study of a small-scale standing-wave thermoacoustic engine. Journal of Mechanical Engineering Science, Vol. 224, 2010.

[9] Smoker, J., M. Nouth, O. Aldraihem, and A. Baz. “Energy harvesting from a standing wave thermoacoustic-piezoelectric resonator.” Journal of Applied Physics, Vol. 111, 2012.

[10] Wheatley, John, T. Hofler, G. Swift, and A. Migliori. “Understanding some simple phenomena in thermoacoustics with applications to acoustical heat engines.” American Journal of Physics, Vol. 53, 1985.

[11] Raspet, Richard, Henry E. Bass, and W. Pat Arnott. “Theoretical and Experimental Study of Thermoacoustic Engines.” The Office of Naval Research, 1992.

[12] Symko, O. G., E. Abdel-Rahman, Y.S. Kwon, M. Emmi, and R. Behuin. "Design and development of high-frequency thermoacoustic engines for thermal management in microelectronics." Microelectronics Journal, Vol. 35, 2004.

[13] Chen, Reh-Lin, and Steven L. Garrett. "Solar/Heat Driven Thermoacoustic Engine." Journal of the Acoustical Society of America, Vol. 103, 1998.

[14] Buda-Ortins, Krystyna. "Prototype Design for Thermoacoustic Flashover Detector." *Master's Thesis*, 2012.

[15] Omega. "One-Piece Mica-Insulated Band Heater." [Data Sheet] Omega Engineering, Inc.

[16] Jin, Tao, Bao-sen Zhang, Ke Tang, Rui Bao, and Guo-bang Chen. "Experimental observation on a small-scale thermoacoustic prime mover." Journal of Zhejiang University SCIENCE A, 2007.

[17] Hamburger, Kenneth, Amr Baz, and Marino di Marzo. "Firefighter Smart Garments for Burn Mitigation and Firefighter Safety." University of Maryland Center for Fire Fighter Safety Research and Development, 2012.

[18] Nouh, Mostafa. "Thermoacoustic-Piezoelectric Systems with Dynamic Magnifiers." Ph. D. Dissertation, University of Maryland, College Park, 2013.

[19] Adapted from the Wikimedia Commons file "Thermo-acoustic cooling machine.png" http://commons.wikimedia.org/wiki/File:Thermo-acoustic_cooling_machine.png#mediaviewer/File:Thermo-acoustic_cooling_machine.png

[20] Symko, Orest. "Energy Conversion Using Thermoacoustic Devices." 18th International Conference on Thermoelectrics, 1999.

[21] Adapted from the Wikimedia Commons file "Heat_Pipe_Mechanism.png" http://commons.wikimedia.org/wiki/File:Heat_Pipe_Mechanism.png